

An Infrared Coronagraphic Survey for Substellar Companions

Patrick J. Lowrance¹, E. E. Becklin², Glenn Schneider³, J. Davy Kirkpatrick⁴, Alycia J. Weinberger⁵, B. Zuckerman², Christophe Dumas⁶, Jean-Luc Beuzit⁷, Phil Plait⁸, Eliot Malumuth⁹, Sally Heap⁹, Richard J. Terrile¹⁰, Dean C. Hines¹¹

ABSTRACT

We have used the F160W filter (1.4 – 1.8 μm) and the coronagraph on the Near-InfraRed Camera and Multi-Object Spectrometer (NICMOS) on the Hubble Space Telescope (HST) to survey 45 single stars with a median age of 0.15 Gyr, an average distance of 30 pc, and an average H-magnitude of 7 mag. For the median age we were capable of detecting a 30 M_{Jupiter} companion at separations between 15 and 200 AU. A 5 M_{Jupiter} object could have been detected at 30 AU around 36% of our primaries. For several of our targets that were less than 30 Myr old, the lower mass limit was as low as a Jupiter mass, well into the high mass planet region. Results of the entire survey include the proper motion verification of five low-mass stellar companions, two brown dwarfs (HR7329B and TWA5B) and one possible brown dwarf binary (Gl 577B/C).

Subject headings: stars:low-mass,brown dwarfs

1. Introduction

Just over a decade ago substellar astronomy exploded in discoveries with the first brown dwarfs in the Pleiades (Rebolo, Zapatero Osorio & Martin 1995), the first ‘cool’ brown dwarf, Gl

¹Spitzer Science Center, MS 220-6, California Institute of Technology, Pasadena, CA. 91125; lowrance@ipac.caltech.edu

²University of California Los Angeles, Los Angeles, CA

³University of Arizona, Tucson, AZ

⁴Infrared Processing and Analysis Center, California Institute of Technology, Pasadena, CA

⁵Carnegie Institution of Washington, Department of Terrestrial Magnetism, Washington, DC

⁶European Southern Observatory, Santiago, Chile

⁷Laboratoire d’Astrophysique, Observatoire de Grenoble, France

⁸Sonoma State University, Rohnert Park, CA

⁹NASA, Goddard Space Flight Center, Greenbelt, MD

¹⁰Jet Propulsion Laboratory, Pasadena, CA

¹¹Space Science Institute, Boulder, CO

229B (Nakajima et al. 1995), and the first extrasolar planet (Mayor & Queloz 1995). The added identification of hundreds of field brown dwarfs in large scale surveys such as 2MASS (Skrutskie et al 1997) and SDSS (York et al 2000) led to the creation of two new spectral types, L and T (Kirkpatrick et al 1999; Burgasser et al 2002; Geballe et al 2002).

Brown dwarfs occupy the important region in the mass range between stars and planets. Their existence and properties give insight into stellar and planetary formation. They are thought to form like stars, but do not have enough mass to sustain hydrogen fusion. With low temperatures and compact atmospheres different from stars, the lowest-mass brown dwarfs should resemble the higher mass giant planets. The observational distinctions between a planet and brown dwarf at the low mass end have yet to be constructed except that a 'planet' should be a companion to a star.

To fully explore the similarities and differences of stellar and planetary formation, brown dwarfs as companions are essential. Since the brighter primary's age and distance are known, these two properties that are usually uncertain for field brown dwarfs are already established for companions. Therefore companions can be standards and anchor models as the multiplicity fraction, separation distribution, and mass ratio distribution of companions provide important hints as to formation mechanisms. Radial velocity surveys find that about 5% of G stars have massive Jupiter planets within 5 AU, but that brown dwarfs are rare (<0.1%) at these separations. Even though Gl 229B is a companion to an M star, many earlier companion searches have turned up few discoveries. Closer looks at the younger cluster and field brown dwarfs have found several to be equal-mass binaries (Zapatero-Osorio, Martin, & Rebolo 1997; Koerner et al 1999; Reid et al 2001). About 20% of field L dwarfs have been shown to be binaries with projected separations < 20AU while closer to 45% of L dwarf companions to stars are actually binaries (Burgasser, Kirkpatrick, & Lowrance 2005). The frequency of brown dwarf companions might be dependent on mass and separation (Gizis et al. 2001), but these ideas need a larger sample to be explored.

The primary goal of this survey was the discovery of substellar companions to young, nearby stars. Here we present results from our infrared coronagraphic survey with the Near-Infrared Camera and Multi-Object Spectrometer (NICMOS) on the Hubble Space Telescope (HST), including follow-up adaptive optics observations obtained at the Canada-France-Hawaii Telescope (CFHT) and 200in Hale Telescope and spectra obtained with the Space Telescope Imaging Spectrograph (STIS). Previously, this survey presented TWA5B, a ~ 20 Jupiter mass brown dwarf companion (Lowrance et al. 1999) and HR 7329B, a ~ 40 Jupiter mass brown dwarf companion (Lowrance et al. 2000). The full survey results along with six additional discoveries are presented here.

2. Defining the Sample

As part of the ISO Debris project to detect dust around main sequence stars, a list of young, nearby stars was assembled. The list was expanded to include young objects selected through techniques including chromospheric activity, the presence of lithium, and space motions as discussed

later. Typically, the systems selected were young, single stars within ~ 50 pc of the Sun. Since brown dwarfs are relatively dim, younger and closer ones should be brighter, and therefore easier to detect.

Brown dwarfs and giant planets are more luminous when they are young due to gravitational contraction energy remaining from formation. Models of substellar objects show that $L \sim t^{-1.3} M^{2.24}$, where L is luminosity, t is age and M is mass, based on cooling curves using atmospheric physics (Burrows et al. 1997). Since models predict the bolometric correction at H-band does not change much for cool temperatures below 3000 K, we can expect a similar relation for an object’s H-band flux as a function of mass and age. If atmospheric models are correct, we expect a $5 M_{Jupiter}$ object to have a $M_H \sim 17.5$ mag at 10^8 years (Burrows et al. 1997).

2.1. Building the Target List

As part of the NICMOS Instrument Definition Team (IDT), the EONS team (Environments of Nearby Stars) was awarded guaranteed time of approximately 80 orbits on the Hubble Space Telescope, of which 50 were dedicated to finding brown dwarfs around young stars (HST Program ID 7226, 7227). The team prioritized the list of stars to the “fifty best” targets, attempting to maximize the probability of discovery. The three main factors that were taken into account include lack of binarity, close distance, and young age.

A close ($<20''$) binary significantly lowers the probability of another companion being in a close, stable orbit (within a few arcsec) to the star. Triple systems with a ratio of major axes < 5 are thought to be unstable (Harrington 1977). All known close binaries were left off the target list, but since many of the apparently single stars had never been observed with at high resolution, some stellar binaries were still to be expected.

At a distance of 50 parsecs, objects discovered at $0''.4$ (coronagraphic radius = $0''.3$) would be 20 AU from the primary star. This is near the maximum in distribution of separations of binaries in Duquennoy & Mayor (1991). Most of the distances for the targets are determined from the Hipparcos mission data, and are accurate to a few percent. Some of the stars were not observed by the Hipparcos mission and the photometric distance is used. The distribution of distances peaks near 30 parsecs, the median distance of the sample. The minimum observable separation of 12 AU, at 30 pc, is inside the average orbital distance of giant planets in our solar system. A few stars selected for this project were farther than 50 parsecs but were chosen because of their extreme youth (e.g., TW Hydrae Association).

There are many stars within ~ 50 pc of the sun with ages similar to or less than the age of the Pleiades ($t=125$ Myr, Stauffer, Schultz, & Kirkpatrick 1998). Youth can be inferred observationally in a number of ways. These different age determinations can be intercompared. One method is measuring photospheric lithium abundance in stars later than $\sim K5$ in spectral type. This fragile element is destroyed at temperatures greater than 2×10^6 K and convective motions within a late-

type star’s layers will, within less than a hundred million years for $0.1M_{\odot}$ stars, cycle all lithium to the hot core. Studies of stars in clusters (Favata et al. 1993) have shown that at a given spectral type, lithium abundance decreases as a function of age, where age can be determined independently from other means, such as main-sequence fitting.

Another method to determine age is measurement of coronal or chromospheric activity such as $H\alpha$ emission, Ca H & K line emission, and X-ray emission. All of these are coupled to rotational velocity and magnetic field activity, presumably a result of the internal dynamo. Stars typically spin up to high rotational velocities ($> 200\text{km s}^{-1}$) when young and slow down as angular momentum is lost through stellar winds. A problem with this method on an individual star basis is that close binaries with periods less than a few weeks are often tidally locked and maintain high levels of activity regardless of age.

Main-sequence fitting is another useful method which places stars on an H-R diagram and compares their location to clusters of approximate ages. Accurate distances of field stars became available as a result of the Hipparcos mission, and main-sequence fitting became much more effective in the age determination. One method of age determination is kinematics, in which comparisons are made between a star’s galactic motion and that of clusters of approximate ages. This proves successful in providing a general age-group for individual stars.

Age estimates for our sample are found using an intercomparison of lithium abundance, coronal & chromospheric activity, rotational velocity, main-sequence fitting, and kinematics (Appendix A). Upper limits and lower limits are calibrated against samples of T Tauri stars (~ 1 Myr) and stars in young, nearby clusters such as the Pleiades (125 Myr), Ursa Major (300 Myr) and the Hyades (600 Myr).

The original plan was to re-observe all frames containing point-sources within three to four years for proper motion confirmation of companionship. However, it was learned after launch that NICMOS would have a shorter lifetime than expected due to coolant problems. Chance for follow-up was now limited to within two-years with NICMOS or from ground based telescopes. To limit the number of extraneous background stars, we therefore excluded most target stars with $|b| < 15$ deg.

The final sample (Table 1) consists of 45 single stars with a median distance of 30 parsec and median age of 0.15 Gyr. The sample was concentrated toward cooler spectral types (Figure 1) mainly for contrast considerations, because faint substellar companions will be easier to detect near fainter primaries. They were observed as scheduled from 18 Mar 1998 to 18 Dec 1998.

3. Observations

3.1. Using NICMOS: An Infrared Instrument Aboard the Hubble Space Telescope

The main problem with trying to image brown dwarfs or giant planets around main-sequence stars is the overwhelming brightness of the primary. A substellar companion will be much fainter than the star it orbits (i.e. a Gl 229B-like object, $L=2\times 10^{-5}L_{\odot}$, orbiting a solar-like star of $1 L_{\odot}$). The cool brown dwarf makes up a little of this in the infrared, where it radiates much of its light, and is brighter with youth, but the primary is still much brighter. According to theory (Burrows et al. 1997), Gl 229B was 50 times, or 4.25 mag, brighter at 10^8 yr old. Also, formation theories of high mass planets predicted orbits very close to its primary, as well, so high resolution, achievable from space, was essential. The Near-Infrared Camera and Multi-Object Spectrometer, NICMOS, is a second-generation instrument for Hubble Space Telescope. NICMOS has three available cameras. Camera 2 has a $\sim 19''\times 19''$ field of view with $0''.076$ pixels and provides higher resolution and image stability than ground based instruments. Most importantly, the coronagraph on camera 2 is actually a hole in the field divider mirror that is baffled with a cold pupil plane mask (Thompson et al. 1998), and therefore can provide higher sensitivity to faint companions than direct imaging (and PSF subtraction) because of the actual reduction of light in the optical path.

We conducted the survey at F160W, which corresponds roughly to the H-band filter on the ground. There are three main reasons for choosing this filter. First, the dominant sources of background radiation are the zodiacal light at short wavelengths and the thermal background emission from the telescope at long wavelengths. The sum of these two components are a minimum at $1.6\mu\text{m}$ (see Table 4.8 of the NICMOS Data Handbook). Second, in camera 2 the PSF is Nyquist sampled at $1.67\mu\text{m}$ and $\sim 90\%$ of the light of the primary is contained within the coronagraph which has a $0''.6$ diameter. Because the coronagraphic hole was baffled, it reduced the amount of light from the primary by a factor of 6 at $1''$ compared to direct imaging (Schneider et al 1998). Finally, there are two main filters on Camera 2 which could have been used, F165M ($1.55\text{--}1.75\mu\text{m}$) and F160W ($1.4\text{--}1.8\mu\text{m}$). There was a question which of these would be more useful in detecting very cool objects ($T < 1000\text{K}$) because of the presence of methane absorption at H-band. Using the spectrum of Gl 229B, a comparison of the filters found that, a similar flux and temperature object would have 1.6 times greater signal to noise ratio in the wider filter. Therefore, we conducted our imaging survey on Camera 2 with the coronagraph at F160W.

In target acquisition the centroid of the target's PSF is placed at the 'low-scatter-point' of the hole by an on-board acquisition. It is slightly different from the center (-0.75 pixel in X and -0.25 pixel in Y) to optimize stray light rejection determined by in-flight testing of the NICMOS IDT. (Schneider et al. 2001). Our choice of the centration points within the coronagraphic hole was designed to reduce the intensity of the speckle pattern from the optics at the edge of the hole.

With the target behind the coronagraph, we reduce the amount of light in an azimuthal average at the edge of the coronagraph compared to direct imaging allowing for deeper investigation for

companions. We developed an observing strategy to go even deeper, as explained below.

3.2. Roll Subtraction

The Hubble telescope has the ability to slew in three ways: in x , in y , and in θ . In order to keep the target star in the same position behind the coronagraph, as well as simplify the removal of the stellar profile, we designed two observations of the star at different spacecraft orientations ($\delta\theta$) separated by 29.9 degrees¹. This was the maximum roll the telescope could maintain and still keep its solar arrays pointed toward the sun. For a companion 0''.5 from the star, a 26 degree roll is the minimum needed for the two PSF's (the companion's PSF at the two roll angles) to be separated by a distance equal to their first Airy maxima. Therefore, the observing strategy is to place the star behind the coronagraph, observe for about 800s, roll the telescope, and observe again for 800s. This integration time kept both rolls to fit into one orbit, allowing for the roll and second target acquisition. Actual integration times per observation varied from 42s to 256s depending on the brightness of the primary (saturation at 0''.4 was avoided) with multiple frames adding up to \sim 800s). The 800s was typically split into at least three Multi-Accum (non-destructive read) integrations (MacKenty et al. 1997).

This helped reduce intrinsic detector non-linearities and lessened the chance of saturating pixels at small angular distances from the occulted core of the target PSF. It also made maximum use of the available dynamic range. When we subtract the two images, the background from the star should ideally subtract out and if there are any objects in the field, two images of each should remain (Figure 2). Because of thermal induced changes in the telescope (or 'breathing') the HST+NICMOS PSF varies on close to an orbit timescale (even slightly within an orbit) and so scattered light residuals persist as the 10% of the light not contained in the coronagraph will change slightly (Schneider et al. 2001). Therefore, observing at two rolls within an orbit minimized these changes.

3.3. Reduction of NICMOS data

The NICMOS coronagraphic images were independently reduced and processed utilizing calibration darks and flat-fields created by the NICMOS IDT (Instrument Definition Team) from on-orbit observations, rather than library reference files prepared by STScI. Mainly, flatfields were augmented with renormalized data from contemporaneous lamp calibration images (obtained as part of the acquisition process) to help remove artificial edge gradients and allow for calibration directly around the coronagraphic hole (Schneider et al. 2002). Using the NICRED program (McLeod 1997), the observations were bias and dark subtracted, corrected for non-linearities using the ramp

¹A few observations were made at $\delta\theta < 29.9$ due to lack of sufficient guide stars at both orientations

of the multiaccum imaging mode, and flat-fielded. Bad pixels were masked in the calibration steps and replaced with values interpolated from neighboring pixels with a cubic spline function. The three calibrated images at each orientation were then averaged to create final images.

As a final step, the cleaned calibrated images from each of the two spacecraft orientations were subtracted from each other leaving lower amplitude residual noise near the coronagraphic hole edge, as well as positive and negative conjugates of any objects in the field of view (Figure 2). Registration of the images was done 'by-eye' for the smallest residuals as the second image's position was changed by 0.05 pixel in the X and Y directions. It was found early on that the diffraction spikes were never quite aligned in the best azimuthal subtraction, and 'by-eye' ultimately led to the best subtraction. A significant component of the residuals in the diffraction spikes arise in a small misalignment of the image of the mirror support structure formed in the pupil plane and small shifts of the pupil mask itself over time, inducing a diffraction of the spikes themselves (Schneider et al. 2001). The difference image, therefore, produces a 'triple' diffraction spike that varies in amplitude and phase, but has nothing to do with centration.

Since the target star is occulted in the coronagraphic images, its position to measure offsets of possible companions must be ascertained indirectly. First, the target's position was found in the acquisition image by a least-squares isophotal ellipse fitting process around the PSF core with a radius of 7 pixels to exclude flux from any close objects. The target placement in the coronagraphic frames was then determined by applying the target-slew vectors used by NICMOS, accessible from the HST engineering telemetry, resulting in independent measurements of each offset and position from both orientations.

4. Point-Source Detection

4.1. Determining Detection Limits

For a full analysis of the results, it is necessary to determine sensitivity to point sources. To determine the limits at which sources could be detected within the NICMOS roll-subtracted images of the observed stars, we planted² point-spread-function (PSF) stars, generated with Tiny Tim (Krist & Hook 1997), at random locations in every image. These PSF stars are noiseless, and can be adjusted in flux. We examined a range of magnitudes from H=10–22, stepped by 0.2 mag, for each roll subtraction. For each magnitude, 25 stars were planted randomly within 3'' of the center of the primary. This number of stars was chosen to avoid confusion between planted PSF's. For better statistics, it was repeated 40 times for a total of 1000 planted PSF's at each magnitude. Each of the 40 images was cross-correlated with the Tiny Tim PSF to locate planted sources. The values in the correlation map range from 1 for perfectly correlated points to -1 for

²software courtesy of A. Ghez and A. Weinberger.

perfectly anticorrelated points. The results are then compared with the log of the actual planting, and the correlation coefficients of the planted stars are recorded, binned, and averaged as a function of radius. Correlation coefficients of 0.9 or above are treated as definite detections. This limit was very conservative set by the level above which no false hits (glints, etc) were found for several test images. As a test, two observations with candidate companions in the field were also placed through the routine; one with a H=17 ($\Delta m=9.5$) object at $2.5''$ and one with H=20 ($\Delta m=13$) object at $2.5''$. The brighter object was found with a correlation of 0.99, while the fainter was found with correlation of 0.93. The routine found nothing else in each image with a correlation greater than 0.9. The separation from the star at which the correlation reaches 0.9 is then recorded for each magnitude step.

The F160W filter is $\sim 30\%$ wider than ground-based Johnson H-band filters which necessitates a careful conversion from F160W to H band for cool temperature objects. For six M dwarfs between spectral types M6 and M9 with measured F160W and ground-based H-band magnitudes, we find a mean difference of 0.03 mag. Objects with a spectrum like Gl 229B, displaying methane absorption, have a H–[F160W] color of about 0.2 mag. The quoted H magnitudes of objects less than $80 M_{Jupiter}$ are uncertain by 0.25 mag due to uncertainties in the opacities and gravity dependence of methane absorption (A. Burrows, pers comm).

In figure 3, we plot the detection limits found overall in the observations. Our sample has an average primary magnitude $H = 7$ mag and a median age of 0.15 Gyr. At $1''$, we can confidently detect a delta magnitude of 9.5 mag for all stars. At a median distance of 30 pc, $1''=30$ AU and our average limit corresponds to $M_H = 14.1$ mag. From the models of Burrows (pers comm), this corresponds to less than $20 M_{Jupiter}$. The most distant stars are the TWA association, in which $1''$ correlates to 50 AU, but they are much younger (10 Myr), so the detection limit is down at a few $M_{Jupiter}$. At $0.5''$, we can detect a delta magnitude of 7 mag, approximately 3 mag better than most speckle imaging programs (i.e. Bouvier, Rigaut, & Nadeau, 1997; Patience et al 1998).

This program fully sampled 45 young stars with a median age of 0.15 Gyr with the ability to detect $30 M_{Jupiter}$ brown dwarfs. For several of the younger stars we were able to probe deeper in the mass range to only a few $M_{Jupiter}$. For the median distance of 30 parsecs, our search covered 12-120 AU in orbital separation. This covers the maximum of the distribution of companion separations found in the open clusters Pleiades, Alpha Persei and Praesepe, the G-dwarf radial velocity study and observations for T Tauri stars (Patience, J. 1999).

4.2. Detectability of high-mass planets

At large separations from the primary, we were able to detect objects into the high mass planet range. For our oldest stars, $t=0.3$ Gyr, a $5 M_{Jupiter}$ object is expected to have a absolute H mag of 18.7 mag (Burrows, A. pers comm). Outside of $5''$, for the majority of stars, detection was limited by the sensitivity of the images, [F160W] ~ 22 , set by the integration time, so a $5 M_{Jupiter}$ object

was detectable for primaries at 30 parsecs. Closer than $5''$ detectability depends on the brightness, age, and distance of the primary. Using absolute H magnitudes of a $5 M_{Jupiter}$ object of 14.2, 16.7, and 18.7 mag, at the ages of 0.02, 0.1, and 0.3 Gyr, respectively, we plot the number of primaries in which a detection was possible at separations of 30, 50, and 100 AU (Figure 4). This survey could have detected a high mass planet above $5 M_{Jupiter}$ around 36%, 61%, and 80% of the 46 primaries at 30, 50, and 100 AU, respectively.

Radial velocity surveys have found $\sim 6\%$ of the over 1000 FGKM stars have high mass planets within a few AU (Marcy et al. 2004). Since Jovian planets are thought to form at larger distances, several theories have been proposed to explain how these massive planets are so close to their stars. One mechanism proposed (Lin & Ida 1997) is that multiple planets forming within a disk interact gravitationally to kick one planet to an eccentric orbit inside 1 AU, seen in radial velocity studies, while causing another to be ejected to much larger radii (>50 AU).

It is not a strong constraint, but for the 45 stars this program observed, detecting 1–2 high mass planets at large radii would be consistent with all of the radial velocity planets having formed in the interaction method described above. However, it is not possible with the imaging data at a single epoch to distinguish between objects formed in situ or those kicked out.

5. Identification and Analysis of Point Sources

In Table 2 we present the results of point sources identified in the coronagraphic survey. ‘Stellar-like’ candidates are those that have a FWHM between $0''.14$ and $0''.18$, and usually show an Airy diffraction pattern. The high resolution of the observations makes it easy to distinguish between stars and diffuse background galaxies. Several of the candidate companions have been re-observed for proper motion and spectra to confirm companionship and their possible substellar nature. Many candidates were very close to their primaries and had to be followed up with other space-based observations or adaptive optics. In the next sections we will describe the further observations on the candidates that confirmed their background nature or companionship.

5.1. Observations

STIS

The candidate secondaries around HD 177996, TWA 5, HR 7329, GL 577, HD 102982, and GL 503.2 were observed between March and July 2000 with STIS (Program 8176). Each primary was acquired into the $52'' \times 0''.2$ slit and then offset based on the NICMOS astrometric results to place the secondary into the slit. To keep the primary as far out of the slit as possible, we employed a slit position angle so that the line joining the primary and secondary was approximately perpendicular to the slit, thereby minimizing contamination from scattered primary light. Spectral imaging

sequences were completed in one orbit per star with the G750M grating in three tilt settings with central wavelengths of 8311, 8825 and 9336Å (resolution $\sim 0.55\text{Å}$). For HR 7329B, HD177996, Gl503.2B and HD 102982B we integrated for 684s, 344s, and 310s respectively at the three tilt settings and for GL 577B and TWA 5B the integration times were 340s, 172s, and 174s. For TWA 5B and Gl 577B, we obtained flat fields after each set of four spectral images. These were recommended by the STIS team to calibrate the known effects of fringing which appear longward of $\sim 7500\text{Å}$. After our first sets of medium resolution spectra were reduced, the library flats served as well as these contemporaneous flats shortward of $\sim 9000\text{Å}$. For the rest of the observing program, we used library flats and no longer took flat fields on-orbit. This allowed more time for integration in the later spectra. At each tilt setting we executed a two position dither of $0''.35$ along the slit to allow replacement of bad or hot pixels, and the exposures were split for cosmic ray removal. Thus, we obtained four spectra at each tilt setting.

CFHT

The Gl 577, Gl 503.2 systems were observed on 4 and 5 Mar 1999 UT, and HD 180445 was observed 11 Nov 2000 with the Canada-France-Hawaii Telescope (CFHT) using the adaptive optics (AO) system PUEO (Rigaut et al. 1998) and its 1024x1024 HgCdTe Hawaii detector KIR (Hodapp et al. 1994). PUEO delivers diffraction limited images at near-infrared wavelengths (PSF FWHM of 95, 110 and 140 mas for J, H and K bands respectively). KIR is used at the F/20 output focus of PUEO and is sensitive in the $[0.7-2.5]\mu\text{m}$ range. Despite poor meteorological conditions, with cirrus covering most of the sky and an uncorrected seeing varying between $0''.9$ and $1''.5$ over the nights, PUEO was able to easily detect the bright companions of HD 180445, Gl 577, and Gl 503.2 in a single exposure of a few seconds. All three systems were imaged in the J and K bands.

After correction for bad pixels and flat-fielding procedures, we subtracted the sky background. For this purpose, a series of images was obtained for each filter by placing the science target near the center of each of the detector quadrants. The images were co-added, and the sky background was derived from the median of this set of four images.

Palomar

The stars Gl 577 and Gl 503.2 were observed on 14 May 2000 UT, and the stars RE0723+20, GL 875.1, and GL207.1 were observed on 26 September 2000 UT with the 200 inch Hale telescope at Palomar Observatory using the AO system PALAO and its 1024x1024 HgCdTe Hawaii detector, PHARO (Hayward et al. 2000). The system mounts at the Cassegrain focus and can achieve resolution of $0''.05$ at K band. Both Gl 577 and Gl 503.2 systems were observed at K band, and Gl 577 was additionally observed at H.

Basic reduction included correction for bad pixels and flat-fielding procedures following the same methods for the CFHT observations. Clouds precluded direct photometric observation against

standards. We measured the separations for each observation of the pairs. Using the neutral density filters for the position of the saturating primary when the secondary is not seen may lead to a larger statistical offset.

Keck

The Gl 577 system was observed on 12 Aug 2000 using the AO system with the slit-viewing camera (SCAM) on NIRSPEC (McLean et al. 1998). The H-band Strehl ratio, as measured on the primary, was 0.16 with FWHM=0".045 in a 10 second exposure.

Due to the small field-of-view of the infrared camera ($5'' \times 5''$), the primary and secondary were observed in different frames, but the adaptive optics atmospheric corrections were made on the primary during the entire observation. Six H-band images were obtained of the secondary pair in sets of 10 coadds of 1 second integrations dithered about the array.

5.2. Analysis of Follow-up Observations

5.2.1. Background Objects

Indeed, when searching for companions, not all point sources will be companions. That was true with several of the objects detected in this survey. They are presented here as a time-saving service for future astronomers.

Candidate companion to LP 390-16 is a background object

Analysis of the roll-subtracted, coronagraphic images of LP 390-16 reveal a stellar-like object at a separation of $1.45'' \pm 0.08$, and a position angle of $226^\circ \pm 1$ with a F160W magnitude of 14.4 ± 0.1 mag.

To determine possible companionship with the primary, the 1954 epoch Palomar Observatory Sky Survey (POSS) digitized plate was examined in which a star (star X) was found located approximately $10'' \pm 1$ at a position angle of 100 ± 5 degrees from LP 390-16, or $10''$ east and $2''$ south. With a 44 year baseline, if the two stars are unassociated, then LP390-16, with a proper motion listed in table 3, should move approximately $9''$ east and $1''.5$ south leaving a separation of approximately $1''.1$ at a position angle of 120 degrees if star X is background. This is close to the detected point source within the errors of measurement on the POSS plates, and the candidate companion was the only object near this position in the NICMOS images. Therefore we conclude the secondary we detect in the NICMOS images is consistent with this same background star. This object is not seen in the second epoch POSS plates, epoch 1993, which could be due to the current proximity of LP 390-16.

Candidate companion to HD 177996 is a background object

A STIS follow-up observation of the candidate companion of HD 177996 was attempted on 27 Feb 2000. In the NICMOS image the $m_H=19.1$ candidate was located at $5.17''$ at a PA of $300^\circ.1$. A spectra of the primary star was obtained, and then at the astrometric offset, a spectra of the secondary was attempted by HST. No detection of the secondary was made in a total exposure time of 10906 seconds with the G750L filter, though the diffraction spikes of the primary are visible at the appropriate separation indicating the offset was performed correctly. HD177996A has a fairly decent proper motion (Table 3) and the NICMOS detection was almost two years earlier (3 May 1998). The half-width of the STIS slit is $0''.1$, so if the candidate companion is a background star it could easily have been at the edge or out of the slit. We therefore conclude the object is a background star and not a companion to HD 177996.

Candidate companion to RE0723+20 is a background object

After the NICMOS observation on 20 October 1998, RE0723+20 was reobserved on 26 September 2000 with the Palomar AO and the closest of the point sources was seen and measured to be separated by $5.4'' \pm 0.1$, and a position angle of $326^\circ.4 \pm 0.4$. With a proper motion listed in Table 3 an object at the original separation and position angle (Table 2) is expected to be at a separation of $5.47''$ and 326° in twenty-three months if it is merely a background object. We conclude this object, therefore, is not a companion. The other two point sources seen in the HST field of view (FOV) were outside the Palomar AO FOV.

Candidate companion to LHS 2320 is a background object

On 01 April 1998, one of the point sources was observed at a separation of $14.92'' \pm 0.11$ and a position angle of $96.9^\circ \pm 0.2$ from the M5 star LHS 2320. Searching the 2MASS point-source database we find two similar sources at the position of LHS 2320 that were observed on 12 Feb 2000 and separated by $16.2''$. With the change in separation over the 1.8 year baseline similar to the primary's proper motion (Table 3), no other point sources in the vicinity of similar brightness, and a J-K = 0.38 mag color, we conclude it is most likely a background G star (10:52:15.3 +05:55:08).

Candidate companion to Gl 875.1 is a background object

After the NICMOS observation on 7 Jul 1998, Gl 875.1 was reobserved on 26 September 2000 with the Palomar AO and the point source was measured to be separated by $7.1'' \pm 0.1$. With the star's proper motion (Table 3), a background object at the original separation and position angle is expected to be at a separation of $6.5''$ and 255° within a time baseline of twenty-three months. We conclude this object, therefore, is not a companion.

Candidate companion to TWA 7 is a background object

TWA 7 was observed with the NICMOS coronagraph on 1998 March 26 with a candidate companion at a separation of $2.44'' \pm 0.05$, and a position angle of $142.2^\circ \pm 0.1$. TWA 7 was also reobserved on 02 November 1998 (Program 7226) with the NIC 1 (pixel scale = ~ 0.043 arcsec pixel $^{-1}$) camera with a medium-band F090M filter (central wavelength: $0.9003 \mu\text{m}$, $\Delta\lambda = 0.1885 \mu\text{m}$). It was observed in a 2 position dither with 4 Multi-Accum integrations of 64s taken at each position for a total of 512s. These were dark subtracted and flat-fielded using calibrations created by the NICMOS IDT.

The F090M filter is a red I-band, covering from $0.8\text{--}1.0\mu\text{m}$. The colors of the possible companion (F090M-F160W=0.72) are consistent with a mid-K star. The candidate was observed with Keck on 20 February 2000 and had changed separation from the primary from $2.44'' \pm 0.05$ to $2.54'' \pm 0.08$ over the almost two year baseline. With the the change in separation and color, we conclude TWA 7 and the candidate were not associated, in agreement with Neuhauser et al (2000a)

Candidate companion to TWA 6 is a background object

A point-source ($H=19.93 \pm 0.08$ mag) was discovered on 20 May 1998 at a separation of $2.549'' \pm 0.011$, and a position angle of 278.7 from the young star TWA 6. The field was re-observed with NICMOS on 2002 June 10. The point source was found to lie at a separation of $2.356'' \pm 0.009$ and a position angle of $281.5^\circ \pm 0.1$ from TWA 6. This change over the 4 year baseline corresponds to a δ (RA,Dec) = $(-52.2, -21.2)$ mas/yr. Webb et al (1999) reported the proper motion of TWA 6 to be $(-60,-20)$ mas/yr, which makes this change in separation wholly consistent with being a background object and not a companion object.

The field of TWA 6 was reobserved with the NICMOS 1 camera on 09 December 1998 (Program 7226) with a medium-band F090M filter and the point source was not detected. We derived an upper limit (3σ) to the flux of [F090M]=22.6 mag in the predicted position from the NICMOS images. Using low-temperature models to transform between F090M and I-band, we calculated an upper limit of $I-H > 3.3$ for the candidate companion. We conclude the object is a very red background object, nonetheless.

5.2.2. Confirmed Companions

In this section, we discuss several positive confirmations from this survey. Two of the discoveries, TWA 5B and HR 7329B have already been presented in L99 and L00 respectively. Independent proper motion confirmations for TWA 5B, HR 7329B and GL 577B have been presented in Neuhauser et al (2000b), Guenther et al. (2001) and Mugrauer et al. (2004). We present the results of the follow-up observations for TWA 5B and bright point sources around other stars with fairly well-known ages.

Bright companions near HD180445, HD 220140 and HD160934

Analysis of the subtracted, target-acquisition images of HD 180445 observed on 27 August 1998 reveal a stellar-like object at a separation of $9.45'' \pm 0.08$, and a position angle of $52.5^\circ \pm 0.5$. On 11 November 2000, the point source was re-observed at $9.5'' \pm 0.1$ and a position angle of $53.0^\circ \pm 0.8$ in the 0.5s acquisition image before acquiring HD 180445 behind the coronagraph on CFHT. The proper motion of HD 180445 (Table 3) should have changed the separation in two years by $0.27''$ if it was a background object. From the 2MASS database we find a point-source at a separation of $9.47'' \pm 0.02$, and a position angle of $53.0^\circ \pm 0.1$. From both of the observations and the 2MASS observation, we conclude that this pair is most likely a common proper motion pair within the errors. The 2MASS magnitudes of HD180445A are $J=6.99 \pm 0.02$ mag, $H=6.49 \pm 0.03$ mag, and $K=6.38 \pm 0.02$ mag, while the magnitudes of HD180445B are $J=10.46 \pm 0.04$ mag, $H=9.88 \pm 0.04$ mag, and $K=9.69 \pm 0.03$ mag. The J-K color of 0.77 and derived absolute magnitudes are consistent with an early to mid-M star.

A point source was found at a separation of $10.85'' \pm 0.08$, and a position angle of $216.3^\circ \pm 0.5$ from HD 220140 when it was observed with NICMOS on the 25 October 1998. From the 2MASS database 8 Oct 2000, one point source was found within a $15''$ search. The candidate companion is separated by $10.85'' \pm 0.08$ and a position angle of $215.15^\circ \pm 0.05$ from the primary. From the listed proper motion of HD220140 (Table 3) the two should have been separated by $11.20''$ and position angle of 217.5° during the two year baseline if the point source was a background object. Therefore the candidate is most likely a proper motion companion within the errors. The 2MASS magnitudes of HD220140A are $J=5.90 \pm 0.02$ mag, $H=5.51 \pm 0.04$ mag, and $K=5.40 \pm 0.02$ mag. The magnitudes of HD220140B are $J=8.04 \pm 0.02$ mag, $H=7.39 \pm 0.03$ mag, and $K=7.20 \pm 0.02$ mag with a J-K color and derived absolute magnitudes consistent of a mid-M star.

Weiss (1991) detected a second object at $20''$ at a position angle of 150° from HD 160934 which did not change position angle or separation from 1955 to 1990. From the 2MASS database observation on 12 May 1999, one point source is found at $19.06''$ at a position angle of 151.1° from the primary. In the 44 year baseline, with the proper motion of HD 160934 (Table 3), the separation would have increased by at least $1.5\text{--}2''$ if it was not a companion. The 2MASS magnitudes of the companion are $J=10.25 \pm 0.02$ mag, $H=9.67 \pm 0.02$ mag, and $K=9.42 \pm 0.02$ mag with a J-K color ($J-K=0.83$ mag) and derived absolute magnitudes consistent of a mid-M star.

STIS Spectra of Gl 503.2, Gl 577, TWA5B and HD 102982

Observations of four candidates were taken with the STIS instrument to determine if they were background objects or companions. The STIS spectra were calibrated, averaged, binned to a resolution of $\sim 6\text{\AA}$ and normalized to the flux (in $\text{ergs/s/cm}^2/\text{\AA}$) at 8500\AA . We compared the final, total spectra to those of standard low-temperature dwarf star spectra with a resolution = 18\AA , a factor of three lower than our STIS spectra (Kirkpatrick et al. 1991; Kirkpatrick et al. 1997) (see Figure

5). All spectra contain the Na I absorption doublet near 8200\AA which does not appear in late-type giant stars. The TiO absorption bands at 8450\AA and 8900\AA are also used to choose the best fitted standard. As seen in Figure 5, the slopes of the spectra from 8600 to 8850\AA are small and fit the dwarf spectra well. The best fit appears to lie between M4V and M5V for Gl 503.2B, at M5V for HD 102982B, between M5V and M6V for Gl577B and M9V for TWA 5B. (The spectrum for HR 7329B was previously published in L00). The spectral type derived for TWA 5B is consistent with photometric spectral type of $M8.5 \pm 0.5$ spectral type derived by L99 and Neuhauser et al (2000b).

Binarity of the companion to Gl 577A

The companion to Gl 577A appears to be elongated in both the CFHT images, Palomar, and the NICMOS images, suggesting that the companion is in fact a close binary system itself with an angular separation slightly lower than the instrumental resolution (~ 100 mas). The two components were resolved with the Keck system (Figure 6). The measured separation of $0.082'' \pm 0.005$ corresponds to a projected radial separation of < 4 AU, corresponding to a period of approximately 20 years. With periodic observations of these two components including radial velocity measurements, the dynamical mass of this low-mass binary can be determined and used to check current evolutionary models.

Astrometry of the Companions

From the ground based observations, a common proper motion between the primaries and secondaries can be established. The known proper motions for the primary stars are listed in Table 3. For Gl 577 and Gl 503.2 systems, the position of each object was measured in a gaussian centroid in each reduced image from NICMOS, CFHT and Palomar. The separations were then calculated and averaged over all measures for each star at each epoch and plotted over time (Figure 7).

If the secondary is not associated with the primary, then the separation should change in an amount that is calculable from the measured proper motion (Table 3). If Gl 503.2B is not associated with Gl 503.2A, then the separation between them should have changed from $1.557''$ to $1.613''$ from the NICMOS observation until the Palomar observations. Instead, the separation was measured at $1.579''$. This is within the 1 sigma error of the NICMOS measure, but 3 sigma outside of being a background object. We therefore conclude Gl 503.2B is a likely companion of Gl 503.2A.

Similarly, if Gl 577 B & C are not associated with Gl 577A, the separation should have changed from $5.348''$ to $5.176''$ within the 2 years between observations. The separation was measured to be $5.31''$ in the Palomar observations, three sigma above the expected change, and within 1 sigma of the NICMOS measure, leading to the conclusion that GL 577 B & C are indeed companions to Gl 577A.

The separation of HD 102982A and B was measured with NICMOS and again in the STIS acquisition before being placed in the slit. In the STIS acquisition images, before and after centering,

a 2d gaussian was fit to get a separation of $0.943'' \pm 0.002$. A flux-weighted centroid using the DAOPHOT routine received similar results. The position angle between the two components was calculated to be 28 ± 2 degrees. This is within 1σ of the separation and position angle measured from the NICMOS image 2.25 years earlier. The proper motion of the primary should change the separation by $0.21''$, or 10σ , if the B component was not associated, therefore we conclude HD102982B is a companion to HD102982A.

6. Determination of Mass

Mass is the best determinant of the substellar nature of an object. Unfortunately, the current ability to dynamically determine the mass of most these objects is impossible, therefore we must rely on evolutionary models of temperature, radius, and luminosity. To plot these objects on evolutionary tracks, we need the luminosity, or absolute magnitude, and the effective temperature. We have converted NICMOS measured photometry to absolute magnitudes using known distances from the primary, and used STIS spectra when available, and/or 2MASS infrared colors for the bright companions, to determine spectral type and therefore effective temperatures. Therefore, both parameters on an H–R diagram have been determined independently, and have independent errors which are discussed below.

Proper motion has been demonstrated between the components Gl 577 and HD 102982 within this paper. HR 7329 A & B and TWA 5 A & B have been confirmed as a proper motion pair (Neuhäuser et al 2000; Guenther et al 2001). Gl 503.2 A & B are likely associated based on the density of background stars and their measured properties. The luminosities or absolute magnitudes of the secondaries have been derived using Hipparcos measurements of the primary, which have determined distances known to within a few percent. This small error bar is taken into account when placing companions on the diagrams. The parallax distance was measured to the primaries by the Hipparcos mission (Table 2). With a derived H magnitude of 10.45 for Gl 503.2B, and a distance modulus of 2.05, we calculate an absolute H magnitude of 8.38 ± 0.09 mag, with an uncertainty that includes distance errors and NICMOS calibration errors. In a similar manner, we derive an absolute H magnitude of 8.58 ± 0.15 for HD 102982B and 7.83 ± 0.09 for the Gl 577 B & C pair. From the resolved Keck data, we measure a delta mag of 0.1 ± 0.1 for the B and C components, therefore, equal magnitude components will have absolute H magnitudes of 8.58 ± 0.13 mag. The companions to HD 160934, HD220140 and HD180445 have absolute magnitudes of 7.72 ± 0.04 mag, 5.92 ± 0.04 mag and 6.78 ± 0.04 mag, respectively.

6.1. Effective Temperatures

The effective temperatures have been determined from the spectra, taken with STIS, from 8000–9000Å which have several spectral features including bands of TiO and Na which are specific

to low-temperature spectral classes from M4V–M9V. The spectral class assignments based on these absorption features are good to 0.5 spectral type, which is the error we assign. Determining the effective temperature adds the largest error because the relationship between spectral class and effective temperature is largely unknown for late-M type stars. Luhman & Rieke (1998) derive a linear relation based on spectral class from Leggett et al’s (1996) fit to synthetic models which agrees with the newer models produced by Leggett, Allard, & Hauschildt (1998) within an uncertainty of about 100 K. This relation of Luhman & Rieke (1998) was used to determine the temperatures of our candidates’ spectral types and a 100K error bar covers a ± 0.5 spectral type. We calculate 3180K, 3010K, and 2840K for M4 V, M5 V and M6 V respectively. For the brightest companions, HD160934B, HD180445B and HD 220140B, we assumed a spectral type of $M4\pm 1$ from the 2MASS colors and derived absolute magnitudes and get a temperature of $3180\text{K} \pm 200\text{K}$.

With the uncertainty for late M dwarf star temperatures in mind, we plot the derived temperatures for each spectral class (Figure 8) with their derived absolute H magnitudes.

6.2. Derived Mass and Age

From their placement on pre-main sequence evolutionary tracks (Baraffe et al 1998), we can infer a mass for the secondaries (Figure 8). HD 220140B and HD160934B seem to be low mass stars falling near the 10 Myr and 100Myr isochrone, consistent with derived ages (discussed in Appendix A) of their primaries. HD180445B appears to be a young low mass star near 50Myr, younger than the derived primary’s age, which was an upper limit of 200Myr, especially since Soderblom et al. (1998) speculated it might be a tidally locked binary and not young at all. HD 102982B and Gl 503.2B appear to be consistent with very low-mass ($< 0.15 M_{\odot}$) stars falling on the 100 Myr isochrone with error bars extending between about 70 and 300 Myr. This agrees with ages derived for the primaries from other means. Gl 577 B & C appears to lie just on the theoretical brown dwarf mass of $0.08 M_{\odot}$ from its infrared magnitude and spectral type at an age of about 70 Myr with error bars extending 30 and 100 Myr. This has been adjusted by 0.75 mag for being a binary. Since both components are of equal magnitude, this would suggest both might be high mass brown dwarfs separated by ~ 4 AU. The models would also suggest Gl 577 system is younger than the Pleiades (100 Myr) supported by the primary’s chromospheric activity and rotation. Both HR 7329B and TWA 5B are bona fide brown dwarfs with masses of $30M_{Jupiter}$ and $20M_{Jupiter}$ as previously reported (L99;L00).

7. Examining the Companion Mass Function

Even though this survey was originally designed to discover brown dwarfs, we can attempt to examine the companion mass function (CMF), and by extension the IMF, across the stellar/substellar border. Since masses can only be accurately determined for close binaries with

measurable orbits, to derive appropriate masses we use previously quoted models for the discovered companions. In recent studies, in the field (Reid 1999), and the Pleiades cluster (Zapatero Osorio et al. 1997), the relative number of low mass stars and brown dwarfs per log mass interval is consistent with being equal, suggesting a flat initial-mass-function ($\alpha = 1$) for single stars.

Several caveats exist in any statistical examination of a small size sample. We have only examined a small separation range and thrown out all known binaries within $20''$, as mentioned in section 2. Earlier studies in the Pleiades cluster and the field have used hundreds of stars while we have observed just less than 50, which decreases the statistical significance. With these overall limitations in mind, we first estimate what one might expect in detections for our survey, by dividing the mass range into two logarithmically equal bins, $0.03\text{--}0.08M_{\odot}$, and $0.08\text{--}0.2M_{\odot}$. For an approximate idea of how many companions to expect, one can examine statistics within 5 parsecs of the sun. Stars less than $0.2M_{\odot}$ make up approximately 24 of 65 stars (37%) within that distance range. Similar statistics are found in the nearest 100 stars taking into account missing systems. For statistics on the separation range of $30\text{--}120\text{AU}$, one can look at the G-dwarf radial velocity survey and find that $\sim 30\%$ of the stars have companions in that separation range (Duquennoy & Mayor 1991).

From these statistics, we might expect 30% of our stars to have companions at the separations available within this study ($30\text{--}120\text{AU}$), and 37% of those companions to be in the $0.08\text{--}0.3M_{\odot}$ mass bin. Therefore we might expect 11% of our 46 star sample, or 5 companions in this higher mass bin. This study found companions to HD 180445, HD 220140, HD 160934, Gl503.2, and HD 102982 that fit that expectation.

For the brown dwarf range ($0.03\text{--}0.08M_{\odot}$), we have three objects, HR 7329B and Gl 577B & C. For an IMF with an equal mass of stars in equal bins ($\alpha = 2$), we expect about 10 objects in the lower bin, which is not consistent by 3σ with our observations. For a flat IMF ($\alpha = 1$), one which has equal number of stars in each mass bin, we predict 5 objects in the lower mass bin. This is fairly consistent with the findings of this survey, though leans toward an $\alpha < 1$. Therefore, even with the aforementioned caveats, the companion mass function we derive from this survey is consistent with the initial mass function found in the field (Reid 1999) and the Pleiades cluster (Zapatero Osorio et al. 1997).

8. Conclusions

In the last decade, the search for substellar objects has achieved spectacular success with the discovery of the first non-controversial detection of a brown dwarf, the definition of two new spectral types 'L' & 'T', and the uncovering of over 500 L & T dwarfs. Even though observations of field dwarfs can answer many questions about formation and fundamental properties, many questions still exist that can only be answered by observations of brown dwarf *companions*. In order to directly detect substellar companions, we developed an infrared coronagraphic survey of young

stars with the NICMOS camera on HST.

Subtraction of two coronagraphic images taken within the same orbit at two angles of the spacecraft differing by 29.9° was found to produce the most effective method of detecting point sources. For the average primary magnitude of $H=7$ mag, the survey detected a delta mag of 9.5 mag at $1''$ with only the subtraction and no other manipulation of the images. This allowed detection into the high mass planet range at 50 AU from over half of the primaries. Results from this survey include five low mass stars, two brown dwarfs, and one possible binary brown dwarf.

Models play an important role in substellar astronomy, and therefore every substellar companion discovered is extremely important. Because the primaries have been well studied, parameters such as age, distance and metallicities are known and can be used to provide fiducials to refine the present models. For example, the close binary GL 577 B & C presented in this paper can be reobserved over the next few years to derive a dynamical mass to compare other young substellar field brown dwarfs. Higher resolution spectra in the visual and infrared of companions such as TWA 5B and HR 7329B are well constrained with age and metallicity and therefore provide anchors for models. Finally, as more substellar binaries and companions are discovered the parameters can be used as important pointers toward answering the questions of stellar formation versus substellar formation versus planetary formation.

This work was supported in part by NASA grants NAG 5-4688 to UCLA and NAG 5-3042 to the University of Arizona NICMOS Instrument Design Team. This Paper is based on observations obtained with the NASA/ESA Hubble Space Telescope at the Space Telescope Science Institute, which is operated by the Association of Universities for Research in Astronomy, Inc. under NASA contract NAS 5-26555. Some of the data presented herein were obtained at the W.M.Keck Observatory. We would like to thank the invaluable observatory staff at the CFHT, Keck and Palomar Observatories for their assistance. We would like to thank all the people who were helpful references during this study such as R. White, R. Webb, C. McCarthy, and R. Chary. We are grateful to the anonymous referee for a careful review of this manuscript and suggested improvements.

A. Appendix A: Individual Target Ages

A-type stars It is difficult to determine ages for A-type stars, but HR 7329 & HR 8799 appear to be young (< 40 Myr) based on rotation, and more importantly, location on an H–R diagram. For massive stars, rotational velocities decline with age; HR 7329 (A0V) has an especially large $v \sin i$ (= 330 km/s) (Abt & Morrel 1995) which is considerably above the majority of early A-type stars (~ 100 km/s). HR 8799 (A5V) has a moderate $v \sin i$ (= 40 km/s) (Abt & Morrel 1995), and has been spectrally defined as a γ Bootis star (Gray & Kaye 1999) which implies an age of a few to 100 Myr. A color-luminosity relation of nearby young clusters (L00) seems to be correlated for stars of similar age; the 50-90 Myr IC2391 and Alpha Per clusters lie below the older (600 Myr) Hyades and Praesepe. There is a large scatter in the Pleiades (70-125 Myr), which could be due to a range of distances and ages as well as unresolved binaries. HR 7329 and HR 8799 lie on a line located below the Alpha Per and IC 2391 cluster which intersects β Pic, HR 4796 and HD 141569, which suggests that HR 7329 and HR 8799 are between 10 and 30 Myr old (L00). Finally, it has recently been suggested that HR 7329 is a member of a young co-moving cluster (Tucanae) much like the TW Hydrae Association with an age of ~ 40 Myr (Zuckerman & Webb 2000; Webb 2000).

F-type stars HD 35850, HD 209253, & SAO 170610 are believed to be young (<0.3Gyr) due to their rotation activity, lithium abundance and X-ray activity. Tagliaferri et al. (1994) use the Einstein satellite to measure X-ray luminosities of $\log(L_x)=30.0$ erg s $^{-1}$ and 29.7 erg s $^{-1}$ for HD 35850 and HD 209253, respectively. Late F and G type stars in the Pleiades typically have X-ray luminosities of $\log(L_x)=30$ erg s $^{-1}$, while Hyades members fall under $\log(L_x)=29$ erg s $^{-1}$. Tagliaferri et al. (1994) find for HD 35850 and HD 209253 $v \sin i=50$ & 16 km s $^{-1}$ and $\log N(\text{Li}) = 3.2, 2.9$, respectively, by fitting observations with synthetic model spectra. These rotation velocities fall between those of Pleiades members and the UMa Group. The positions of these two late F-type stars ($\log T_{eff} \sim 3.8$) on a Li vs T_{eff} plot is consistent with an age close to that of the Pleiades, but lithium ages for F-type stars are questionable and must be supported with other observations (Favata et al. 1993). The coronal activities (X-rays) and high rotational velocities are consistent with the lithium age of 100-200 Myr. SAO 170610 has a $\log N(\text{Li})=3.75$, which indicates a younger age, between Tau-Aur and Pleiades, or 20–125 Myr. There is also a small measured X-ray flux, ($\log f_x/f_v=-4.15$; Stocke et al. 1991) consistent with a young age.

G-type stars Ten G-type stars were selected based on their chromospheric activity, lithium absorption, and rotation. The flux ratio of Ca II H & K emission to the bolometric flux, or R'_{HK} , and Li abundance, expressed $\log N(\text{Li})$, is compared among stars of young clusters. Henry et al. (1996) selected several stars as “very active” from Ca II emission including HD 202917 ($\log R'_{HK} = -4.06$) and HD 180445 ($\log R'_{HK} = -3.90$). The Ca II H & K ratios imply ages for these objects, if these are single stars, similar to members of the Pleiades cluster, using the chromospheric emission-age relation of Donahue (1993):

$$\log(t) = 10.725 - 1.334R_5 + 0.4085R_5^2 - 0.0522R_5^3 \quad (\text{A1})$$

where t is age in Gyr, and R_5 is defined as $R'_{HK} \times 10^5$. Soderblom, King, & Henry (1998b) measure

a Li abundance in HD 202917 ($\log N(\text{Li})=3.28$) consistent with Pleiades stars of similar spectral type, but measure only an upper limit ($\log N(\text{Li})<1.61$) for HD 180445. Neither star rotates rapidly for G-type stars with $v\sin i=12$ and 8 km s^{-1} for HD 202917 and HD 180445, respectively. Soderblom et al. (1998b) speculate HD 180445 might be a spectroscopic binary. There is the hint of a second pair of spectral lines which could be a tidally-locked secondary causing the chromospheric emission. Therefore the age of HD 180445 is in question, but Soderblom et al. (1998b) conclude HD 202917 is most likely a single, very-active star with an age younger than the Pleiades. Finally, Zuckerman & Webb (2000) suggest HD 202917 is a member of the co-moving cluster, Tucanae Association, with an age of ~ 40 Myr.

HD 105 was identified in Favata et al. (1995) as having a high lithium abundance ($\log N(\text{Li})=3.4$). Using a distance determined by the Hipparcos mission, Favata et al. (1998) re-computed the X-ray flux density measured with the Einstein satellite and find $\log L_x = 29.2 \text{ erg s}^{-1}$, which implies an age a little younger than Pleiades. For reference, the solar X-ray luminosity varies, but is $\log L_x \sim 27 \text{ erg s}^{-1}$. Jeffries (1995) lists a $v\sin i = 13 \text{ km s}^{-1}$ in his sample of active, Li-rich stars.

G1 311 (HD 72905) has a high level of chromospheric activity and rotates rapidly. Soderblom et al. (1985) measure $\log (R'_{HK}) = -4.7$, and Dorren & Guinan (1994) find a rotation period of 4.7 days, from which an age of 300 Myr may be assigned (Kirkpatrick et al. 2001). Recently Gaidos, Henry, & Henry (2000) brought these data together with a Li measure ($\log N(\text{Li})=2.8$), derived (U,V,W) space motions (+18.9,+12.1,-3) and assessed G1 311 belonged to the UMa moving group (+13,+1,-8). From all indicators, it is evident G1 311 is most likely 0.3 Gyr.

HD 220140 (V368 Cep) has been identified as an X-ray source with $\log L_x = 30.5 \text{ erg s}^{-1}$ (Pravdo, White, & Giomi 1985) and light variations with a period of 2.75 days assumed to be due to spots have been measured (Heckert et al. 1990). Chugainov, Lovkaya, & Petrov (1991) find no radial velocity variations over several nights, indicating a single star. They derive space motions of (-22,-28,-4) that are marginally consistent with the Pleiades according to Eggen (1975) (-11,-25,-8). They derive a Li abundance of $\log N(\text{Li})=3.0$ from their spectra, and based on these data give an age of 0.05 Gyr, but it is probably closer to the Pleiades age of 0.125 Gyr from the rotational velocity. Therefore we assign a range from 50-125 Myr.

It has been speculated that G1 503.2 (HD 115043) is a member of the UMa co-moving group based on lithium abundance, kinematics, and chromospheric activity. Soderblom et al. (1993a) compared the abundances of Li in several clusters and found G1 503.2 to lie between the Hyades and Pleiades in abundances for G and K stars. The space velocities (+15,+3,-8) (Rocha-Pinto & Maciel 1998) are similar to the canonical UMa motions. Measurements of Ca II H and K lines ($\log R'_{HK} = -4.43$) and rotational velocity ($v\sin i = 9 \text{ km/s}$) were made by Soderblom & Mayor (1993c). In a solar-like star, such activity is thought to be due to a youthful stage of high magnetic activity. When compared to other stars in Henry et al. (1996), the activity level places G1 503.2 at less than 0.5 Gyr, and is listed with the most active stars in Soderblom et al. (1998a).

Gl 577 (HD 134319) has similar chromospheric emission in the Ca II H & K lines ($\log R'_{HK} = -4.33$) to Pleiades stars (Henry et al. 1996), but its kinematic motions (-33,-15,-1) are more consistent with the Hyades (-40,-16,-3) cluster (Rocha-Pinto & Maciel 1998). Messina, Guinan & Lanza (1999) ascertained a rotation period of 4.448 days from photometric variations thought to be due to dark spots on the surface. They note this rotation period is about half that of most Hyades members, but it does correlate well with UMa group members (Dorren & Guinan 1994). Therefore its age might be as young as 300 Myr, but could be as old as 600 Myr.

HD 70573 and RE 1507+76 are both listed in Jeffries (1995) as active, Li-rich stars with $v\sin i = 11$ & 14 km s^{-1} respectively and Li abundances above Pleiades values with Li (6708Å) EW of 149 & 214 mÅ respectively. Jeffries (1995) derives space motions of (-41,-27,-18) and (-14,-17,-11), respectively. The space motions of HD 70573 are inconsistent with those of Pleiades members, but from the Li and rotation, we conclude that it is a little older than Pleiades at 0.2 ± 0.1 Gyr. RE 1507+76 motions are closer to that of Pleiades members than either those of UMa or Hyades, consistent with the Li abundance and rotation. We therefore assign an age of 0.1 Gyr.

HD 102982 was identified in Henry et al. (1996) as being a highly chromospherically active star due to emission in the Ca II H & K lines ($\log R'_{HK} = -3.86$) giving an age less than Pleiades. Mason et al. (1998) surveyed the most active stars listed in Henry et al. (1996) for multiplicity and found no companions to HD 102982 within 3 mag between 0.035–1.08'' using speckle techniques. Soderblom et al. (1998b) found HD 102982 to be a spectroscopic binary (SB2), and therefore the activity thought to result from youth might instead be caused by the close, less than a few AU, companion. This star (b=9) also slipped past our galactic latitude requirement (b>15) because it was already on the observation calendar when the galactic latitude cut was made.

The presence of the tidally-locked companion to HD 102982 and HD 180445 places their ages in question. Our search with the coronagraph (0.5–4'') covers ~ 20 –150AU at the distance of these stars (42 pc), so we did not expect to image a tidally-locked companion, but rather search for a stable, lower-mass companion farther out.

K-type stars

HD 1405 was identified to have chromospheric emission (Bidelman 1985) and found to have a periodic variation (P=1.7 days) of almost 0.1 mag, indicating rotation of cool spots (Griffin 1992). Pleiades members typically have rotation periods of a couple days. The radial velocity was found to remain constant and that is consistent with the lack of a close companion. Fekel (1997) reports a $v\sin i = 23 \text{ km s}^{-1}$, which agrees with 21 km s^{-1} of Griffin (1992). The rapid rotation and chromospheric emission with lack of a change in radial velocity is consistent with a youthful, single star at 0.1 Gyr.

HD 17925 is of particular interest because it is only 10 pc from the sun. Favata et al. (1995) measured $\log N(\text{Li}) = 2.88$ and $v\sin i < 8 \text{ km s}^{-1}$ in their sample of X-ray active stars. Henry et al. (1996) measure $v\sin i = 6 \text{ km s}^{-1}$, find the H α absorption partially filled in by emission, but conclude that it could be a binary due to line-width variations seen over the three nights they observed.

However, Abbot, Pomerance, & Ambruster (1995) report photometric modulation in a period of 7 days, and a change in the light curve over a three week period consistent with a single, active star. The star has a large $\log R'_{HK}$ ($=-4.30$; Rocha Pinto & Maciel 1998) and Fekel (1997) measures space motions $(-14,-17,-11)$ close to that of the Pleiades, so we assign an age of 0.1–0.2 Gyr.

Lk H α 264 was first identified as an emission line star (Herbig & Rao 1972) and later determined to be a classical T-Tauri star still associated with the Lynds 1457 cloud at only 65 pc (Hobbs, Blitz, & Magnani 1986). Even though it is farther than 50 pc, it is likely a few Myr old star with an H α equivalent width (EW) of 100mÅ (Gameiro et al. 1993). Using several lines of the spectrum, Gameiro et al. (1993) also measured a $v\sin i=22\text{km s}^{-1}$ consistent with a young, late-type star.

HD 21703 was identified in the Einstein survey with a large X-ray flux ($\log f_x/f_{bol}=-2.25$; Stocke et al. 1991), and Favata et al. (1995) measure an upper limit of $\log N(\text{Li}) \leq 1.74$ and $v\sin i=14\text{km s}^{-1}$, placing this mid-K type star near the Pleiades age from these indicators.

Three more K-type stars were selected from Jeffries (1995) study of high activity stars, correlating rotation and H α emission with lithium abundance (Table A1). At this effective temperature, the gap between the Hyades lithium abundance and the Pleiades has widened significantly (Favata et al. 1993), and these objects are near Pleiades age. RE2131+23 and RE 0723+20 also have measured space motions $(-4,-23,-13)$, and $(-6,-27,-15)$ very close to those of the Pleiades, supporting their young ages.

Henry, Fekel, & Hall (1995) present results of photometric monitoring of HD 82443 deriving a period of 5.43 days, and confirm it is single with a constant radial velocity. Fekel (1997) measured a $v\sin i=6.2\text{ km s}^{-1}$, consistent with this earlier measure. With a $\log(R'_{HK})=-4.20$ (Soderblom 1985) and space motions of $(-14,-24,-1)$ (Soderblom & Clements 1987), we conclude this star is probably a little older than Pleiades age. Gl 354.1B is a wide ($65''$), proper motion companion to HD 82443, so we conclude it is of a similar age and add it to our program under M-type stars.

HD 82558 is a chromospherically active, single star. Most main-sequence K-type stars are undetectable at radio frequencies, but Gudel (1992) detected a 3.6cm flux of about 300 μJy and attributed it to gyrosynchrotron electrons in magnetic flux tubes in regions of high chromospheric activity. This star was selected for their study because of the X-ray emission ($\log L_x = 29.1\text{ erg s}^{-1}$) detected in the Rosat All-Sky Survey. Jeffries (1995) lists $v\sin i=25\text{km s}^{-1}$, Li EW = 219 mÅ, and space motions of $(-13,-5,-4)$ consistent with an age of $< 100\text{ Myr}$.

Henry et al. (1995) found photometric variations in Gl 174 (HD 29697) with a period of 3.9 days which they attribute to the presence of spots, deriving a $v\sin i=7\text{km s}^{-1}$. They also measure a H α EW of 200 mÅ and Li EW of 79 mÅ. Using the conversion of Soderblom et al. 1993b, we convert this Li measure into an abundance of $\log N(\text{Li}) = 0.95$. Eggen (1996) observed many low-mass stars and found photometric variations in Gl 174, correlated that with Ca II emission, and concluded that it was 60 Myr old. We conclude from the lithium abundance and chromospheric emission that it is probably closer to Pleiades age, or about 100 Myr old.

Gl 517 (HD 118100) has a high X-ray flux density ($\log L_x/L_{bol}=-3.08$; Sterzik, & Schmitt 1997) typical of young stars approaching the main-sequence, and Favata, Micela, & Sciortino (1997) measure $\log L_x = 29.54 \text{ erg s}^{-1}$ which is consistent. EUV activity and flares were observed from Gl 517 (Tsikoudi & Kellett 1997). Favata et al (1997) measure a Li (EW)=25mÅ and rapid rotation, concluding this star is a BY Dra of a few tens of million years old.

Since Gl 879 (HD 216803) is the common proper motion companion to Fomalhaut, a well-studied A-type star with a debris disk (Holland et al. 1998; Staplefeldt et al. 2004), determination of its age has been very important to disk formation theories. Barrado y Navascues et al. (1997) studied Gl 879 to determine the age of both components placing several factors together. They note the lithium measure of $\log N(\text{Li})=0.6$ makes the star younger than the Hyades but older than Pleiades, while the X-ray activity ($\log L_x = 28.1$; Favata et al. 1997) places the star closer to Hyades age. The rotation ($v \sin i < 4 \text{ km s}^{-1}$) also places the star between the two clusters, but more consistent with the younger Pleiades members, so they conclude an age of $200 \pm 100 \text{ Myr}$ for both Gl 879 and Fomalhaut.

Fekel (1997) finds HD 160934 has a constant radial velocity and a high $v \sin i (=16.4 \text{ km s}^{-1})$. ROSAT detected this star with $\log f_x/f_v = -2.07$ (Schachter et al. 1996) and Henry et al. (1995) measured photometric variability due to spots with a period of ~ 2 days. Therefore, from the rotation and chromospheric X-ray emission, it is most likely a Pleiades age star.

HD 177996 was measured to have considerable Ca II emission ($\log R'_{HK}=-4.17$; Henry et al. 1996), and Soderblom et al. (1998a) derive $\log N(\text{Li})=1.04$, placing the star's age between Hyades and Pleiades. They do find it to be a double-lined spectroscopic binary, but detect lithium in both stars and suggest an intermediate age of 0.5 Gyr.

Jeffries (1995) lists HD 197890 as a very active star with a $v \sin i = 170 \text{ km s}^{-1}$ and $\log N(\text{Li})=3.1$ (Anders et al. 1993). They derive space motions of (-6,-13,+1), similar to the Pleiades. (Favata et al. 1998) measure an X ray activity ($\log L_x=30.2$), consistent with a 100 Myr star.

M-type stars Usually it is a little harder to determine an age for single M-type stars. For example, lithium is destroyed within a few million years in the fully convective interiors and cooler surfaces tend to display a smaller amount of chromospheric activity. We list eight stars selected as the most active, single M-type stars from Reid, Hawley & Gizis (1995) in Table A2 and with higher than normal $H\alpha$ activity, thought to be Pleiades age (Figure A1). The $H\alpha$ EW ranges from 2Å at M0 to 9Å at M5 for the top 10% of Hyades members (Reid, Hawley & Mateo 1995), and from 4Å at M0 to 12Å at M5 for the same tier of Pleiades members (Hodgkin, Jameson, & Steele 1995). Our targets are most consistent with the top members of the Pleiades cluster, suggesting ages of 100 Myr. Some M stars (<10%) have been observed to flare, and any of these measures listed in Table A2 could have been taken during a flare. Therefore we suggest one should be cautious in determining ages from one observational criterion.

Gl 875.1 was detected in EUV flare activity (Tsikoudi & Kellett 1997) and Mathioudakis et al. (1995) measure a rotation period of 1.64 days and $H\alpha$ EW of 3.9Å. The rotation period is

indicative of Pleiades age stars, but the $H\alpha$ is more consistent with an older star, perhaps UMa. Therefore we assign an age of 0.2 Gyr.

TW Hydrae Association Over the last few years mounting evidence has suggested that a number of young, active stars in the vicinity of TW Hydrae form a physical association with an age of ~ 10 Myr (Kastner et al. 1997; Webb et al. 1999; Soderblom et al. 1998c). At an approximate distance of 60 pc, the “TW Hydrae Association” (TWA) is a region of recent star formation nearest to the Sun (Kastner et al. 1997). Webb et al. (1999) added HR 4796A and identified five new systems (seven members), in which each system is characterized by the presence of X-ray emission, $H\alpha$ emission, and strong lithium absorption associated with young stars. The currently identified eleven systems are shown to have similar space motions implying physical association and a possible common origin (Webb et al. 1999). We surveyed 6 of the members, including TWA 1, 5, 6, 7, 8B, and 10 for possible brown dwarf companions. The multiple stars HR 4796A and HD 98800A/B were observed in a sister program for circumstellar disks.

REFERENCES

- Abbot, B.P., Pomerance, B.H., & Ambruster, C.W. 1995 BAAS 27 842
- Abt, H.A., & Morrell, N.I. 1995, ApJS 99 135
- Anders, G.J., Jeffries, R.D., Kellett, B.J., Coates, D. 1993 MNRAS 265 941
- Barrado y Navascues, D., Stauffer, J.R., Hartmann, L., Balachandran, S.C. 1997 ApJ 475 313
- Baraffe, I., Chabrier, G., Allard, F., & Hauschildt, P.H. 1998, A&A 337 403
- Bidelman, W.P. 1985 AJ 90 341
- Bouvier, J., Rigaut, F. & Nadeau, D. 1997 A&A 323 139
- Burgasser, A., Kirkpatrick, J.D. & Lowrance, P. 2005, AJ 129 2849
- Burgasser, A. et al. 2002 ApJ 564 421
- Burrows, A., Hubbard, W. Lunine, J., Marley, M., Huillot, T., Saumon, D., Friedman, R., 1997, ASP Conf. Servies, 119, 9
- Chugainov, P., Lovkaya, M., & Petrov, P. 1991, IBVS 3623 1
- Donahue, R.A. 1993 PhD Thesis, New Mexico State University
- Dorren, J.D. & Guinan, E.F. 1994 ApJ 428 805
- Duquennoy & Mayor 1991, A&A 248, 485
- Eggen, O.J. 1996 AJ 111 466
- Eggen, O.J. 1975 PASP 87 37
- Favata, F., Micela, G., Sciortino, S. & D'Antona, F. 1998 A&A 335 218
- Favata, F., Micela, G., Sciortino, S. 1997 A&A 326 647
- Favata, F., Barbera, M., Micela, G., & Sciortino, S. 1995 A&A 295 147
- Favata, F., Barbera, M., Micela, G., & Sciortino, S. 1993 A&A 277 428
- Fekel, F. 1997 PASP 109 514
- Gaidos, E., Henry, G.W., & Henry, S.M. 2000 AJ 120 1006
- Gameiro J. F., Lago M.T.V.T., Lima N. M., Cameron A. C. 1993, MNRAS 261, 11
- Geballe, T.R. et al 2002 ApJ 564 466
- Gizis, J., Kirkpatrick, J.D. Burgasser, A., Reid, I.N., Monet, D.G., Liebert, J., 2001, ApJ 551 L163
- Gray, R. & Kaye, T. AJ 118 2993
- Griffin, R.F. 1997 Obs 117 208
- Gudel, M. 1994 ApJS 90 743
- Guenther, E. W., Neuhauser R., Huelamo, N., Brandner, W., Alves, J 2001 A&A 365 514
- Harrington, R. S. 1977, AJ, 82, 753

- Hayward, T.L., Brandl, B., Pirger, B., Blacken, C. Gull, G., Schoenwald, J & Houck J.R. 2001 PASP 113 105
- Heckert, P.A., Mooney, C.B., Hickman, M.A., Summers, D. 1990 BAAS 22 837
- Henry, T.J., Soderblom, D.R., Donahue, R.A., Baliunas, S.L. 1996 AJ 111 439
- Henry, G.W., Fekel, F. & Hall, D. 1995 AJ 110 2926
- Henry, T.J. 1991, PhD Thesis, Univ. Arizona
- Herbig, G.H., & Rao, N.K. 1972 ApJ 174 401
- Hobbs L. M., Blitz L., Magnani L., 1986 ApJ, 306 109
- Hodapp, K. W. et al. 1994. Status report on 1024x1024 HgCdTe detector arrays for low-background operation in the 1.0 to 2.5 μm range. Proc. SPIE, 2198, 668
- Hodgkin, S.T., Jameson, R.F., Steele, I.A. 1995 MNRAS 274 869
- Holland, W., Greaves, J.S., Zuckerman, B., Webb, R.A., McCarthy, C., Coulson, I.M., Walther, D.M., Dent, W.R.F., Gear, W.K., Robson, I. 1998 Nature 392 38
- Jeffries, R. 1995 MNRAS 273 559
- Kastner, J.H., Zuckerman, B., Weintraub, D.A., & Forveille, T. 1997, Science 277, 67
- Kirkpatrick, J.D., Dahn, C.C., Monet, D.G., Reid, I.N., Gizis, J., Liebert, J., Burgasser, A. 2001, AJ 121, 3235
- Kirkpatrick, J.D. et al. 1999 ApJ 519, 802
- Kirkpatrick, J.D., Henry, T., & Irwin, M. J. 1997, AJ 113, 1421
- Kirkpatrick, J.D., Henry, T., & McCarthy, D.W. 1991, ApJS 77, 417
- Krist, J. E., & Hook, R. N. 1997, in The 1997 HST Calibration Workshop, with a New Generation of Instruments, ed. S. Casertano (Baltimore: STScI), 19
- Koerner, D., Kirkpatrick, J.D., McElwain, M., Bonaventura, N.R., 1999 ApJL 526 25
- Leggett, S.K., Allard, F., & Hauschildt, P.H. 1998, ApJ 509 836
- Leggett, S.K., Allard, F., Berriman, G., Dahn, C.C., & Hauschildt, P.H. 1996, ApJS 104, 117
- Lin, D. N. C. & Ida, Shigeru 1997 ApJ 477 781
- Lowrance et al. 1999 ApJ 512 L69
- Lowrance et al. 2000 ApJ 541 390
- Luhman, K.L. & Rieke, G.H. 1998, ApJ 497, 354
- MacKenty, J.W. et al., 1997, "NICMOS Instrument Handbook", Version 2.0, (Baltimore: STScI)
- Marcy, G. W., Butler, R. P., Fischer, D. A., & Vogt, S. S., 2004 Extrasolar Planets: Today and Tomorrow, ASP Conference Proceedings, Vol. 321, held July 2003, Institut D'Astrophysique

- de Paris, France. Edited by Jean-Philippe Beaulieu, Alain Lecavelier des Etangs and Caroline Terquem, p.3
- Mason, B.D., Henry, T.J., Hartkopf, W.I., Ten Brummelaar, T., Soderblom, D. 1998 AJ 116 2975
- Mathioudakis, M., Fruscione, A., Drake, J. J., McDonald, K., Bowyer, S., & Malina, R. F. 1995, A&A 300 775
- Mayor, M. & Queloz, D. 1995 Nature, 378, 355
- McLean, I.S. et al. 1998 SPIE Proceedings:Infrared Astronomical Instrumentation, A.M. Fowler; Ed. Vol. 3354, p. 566-578
- Messina, S., Guinan, E. F., & Lanza, A. 1998 Ap&SS 260 493
- Nakajima, T., Oppenheimer, B.R., Kulkarni, S.R., Golimowski, D.A., Matthews, K. & Durrance, S.T. 1995, Nature 378, 464
- Mugrauer, M. et al 2004 A&A 417 1031
- McLeod, B. 1997, in 1997 HST Calibration Workshop, ed. S. Casertano et al., p. 281
- Neuhuuser, R. et al. 2000a A&A 354 9
- Neuhauser, R., Guenther, E. W., Petr, M. G., Brandner, W., Huelamo, N., Alves, J. 2000b A&A 360 39
- Neuhauser, R., Guenther, E. W., Brandner, W., et al. 2000c A&A 360 L39
- Patience, J. 2000, PhD thesis, UCLA
- Patience, J., Ghez, A. M., Reid, I. N., Weinberger, A. J., Matthews, K. 1998 AJ 115 1972
- Pravdo, S.H., White, N.E. & Giomi, P. 1985 MNRAS 215 11
- Rigaut, F., et al. 1998, PASP 110 152
- Rebolo R., Zapatero Osorio M.R., Martin E.L. 1995 Nature 377 102
- Reid, N., Gizis, J., Kirkpatrick, J.D., & Koerner, D. 2001, AJ 121 489
- Reid, N. 1999, "M dwarfs, L dwarfs, T dwarfs and Subdwarfs: $\Psi(M)$ at and below the Hydrogen-Burning Limit" in Star Formation 1999, p327
- Reid, I.N, Hawley, S. & Gizis, J. 1995 AJ 110 1838
- Reid, I.N, Hawley, S., & Mateo, M. 1995 MNRAS 272 828
- Rocha-Pinto, H.J. & Maciel, W.J. 1998 MNRAS 298 332
- Schachter, J., Remillard, R., Saar, S.H., Favata, F., Sciortino, S., Barbera, M. 1996, ApJ 463 747
- Schneider, G., Becklin, E. E., Smith, B. A., Hines, D., Weinberger, A. J., and Silverstone, M., 2001 AJ 121 525
- Schneider, G., 2002, "Coronagraphy with NICMOS", in The 2002 HST Calibration Workshop, eds. S. Arribas, A. Koekemoer, and B. Whitmore, (Space Telescope Science Institute, Baltimore, Maryland), 249

- Skrutskie, M et al. 1997 The Impact of Large Scale Near-IR Sky Surveys, eds. F. Garzon et al., p. 25. Dordrecht: Kluwer Academic Publishing
- Soderblom, D.R. 1985 AJ 90 2103
- Soderblom, D.R. & Clements, S. 1987 AJ 93 920
- Soderblom, D.R. & Mayor, M. 1993 AJ 105 226
- Soderblom, D.R., Pilachowski, C., Fedele, S., Jones, B. 1993a AJ 105 2299
- Soderblom, D.R., Jones, B., Balachandran, S., Stauffer, J.R., Duncan, D., Fedele, S., Hudon, J.D. 1993b AJ 106 1059
- Soderblom, D.R., King, J., Hanson, R., Jones, B., Fischer, D., Stauffer, J.R., Pinsonneault, M. 1998a ApJ 504 192
- Soderblom, D.R., King, J., Henry, T., 1998b AJ 116 396
- Soderblom, D.R. et al 1998c, ApJ 498, 385
- Staplefeldt, K. et al. 2004 ApJS 154 458
- Stauffer, J.R., Schultz, G., & Kirkpatrick, J.D, 1998, ApJ 499 L199
- Sterzik, M.F. & Schmitt, J. 1997 AJ 114 1673
- Stoeck, J.T., Morris, S., Gioia, I.M., Maccacaro, T., Schild, R., Wolter, R., Fleming, T., Henry, J.P. 1991 ApJS 76 813
- Tagliaferri et al. 1994 A&A 285 272
- Thompson, R., Rieke, M., Schneider, G., Hines, D., & Corbin, M. 1998 ApJ 492 L95
- Tsikoudi, V. & Kellett, B. J. 1997 MNRAS 285 759
- Webb, R.A. 2000, PhD thesis, UCLA
- Webb, R.A., Zuckerman, B., White, R.J., Patience, J., Schwartz, M., McCarthy, C. & Platais, I. 1999 ApJ 512 63
- Weiss, E. 1991 AJ 101 1882
- York, D.G. et al 2000 AJ 120 1579
- Zapatero Osorio, M.R., Rebolo, R., Martin, E.L., Basri, G., Magazzu, A., Hodgkin, S.T., Jameson, R.F., & Cossburn, M.R. 1997, ApJ 491, L81
- Zapatero-Osorio, M.R., Martin, E.L., & Rebolo, R. 1997, A&A, 323, 105
- Zuckerman, B. & Webb, R.A. 2000 ApJ 535 959

Table 1. Survey Stars

Primary	other names	α (J2000)	δ (J2000)	m_H	Spec type	D (pc)	b	Approx age (Gyr)
HR 7329	HD 181296	19 22 51.23	-54 25 26.2	5.03	A0V	47.7*	-26	0.01–0.04
HR 8799	HD 218396	23 7 28.72	+21 08 03.4	5.33	A5V	39.9*	-36	0.01–0.04
SAO 170610	HD 37484	05 37 39.63	-28 37 34.6	6.38	F3V	59.5*	+35	0.02 - 0.1
HD 35850		05 27 04.77	-11 54 03.5	5.19	F7V	26.8*	-24	0.1
HD 209253		22 02 32.98	-32 08 01.6	5.53	F6/F7V	30.1*	-53	0.2–0.3
HD 105		00 05 52.56	-41 45 11.5	6.17	G0V	40.2*	-73	0.1
HD 70573		08 22 49.94	+01 51 33.4	7.36	G6V	32	+21	0.2–0.3
GL 311	HD 72905	08 39 11.73	+65 01 15.2	4.25	G1V	14.3*	+36	0.3
GL 503.2	HD 115043	13 13 37.10	+56 42 30.1	5.45	G2V	25.7*	+60	0.3
HD 102982		11 51 09.14	-51 52 32.3	6.96	G3V	~42	+10	0.1 ?
GL 577	HD 134319	15 05 50.16	+64 02 49.8	6.88	G5V	44.3*	+47	0.3–0.6
HD 135363	RE 1507+76	15 07 56.24	+76 12 02.4	7.19	G5V	29.4*	+38	0.1
HD 180445		19 18 12.65	-38 23 04.6	6.84	G8V	41.7*	-21	0.20?
HD 202917		21 20 49.95	-53 02 03.0	7.13	G5V	45.9*	-43	0.04–0.1
HD 220140	V368 Cep	23 19 26.56	+79 00 12.4	5.87	G9V	19.7*	+17	0.05–0.1
HD 1405	PW And	00 18 20.76	+30 57 22.0	7.35	K2V	47.9	-31	0.1
RE 0041+34	QT And	00 41 17.26	+34 25 17.7	6.41	K7V	15.0	-28	0.03
HD 17925	EP Eri	02 52 32.15	-12 46 11.1	4.22	K1V	10.4*	-58	0.1–0.2
LkHa 264	WY Ari	02 56 37.65	+20 05 36.0	10.14	K3V	~65	-34	0.01
HD 21703	AK For	03 29 22.88	-24 06 03.1	6.59	K4V	31.7*	-54	0.1
GL 174	HD 29697	04 41 18.82	+20 54 05.5	5.75	K3V	13.5*	-16	0.06
G 88-24	RE 0723+20	07 23 43.68	+20 25 02.5	7.19	K5V	23.0	+16	0.1
HD 82443	GJ 354.1A	09 32 43.78	+26 59 18.5	5.28	K0V	17.8*	+46	0.2
HD 82558	GJ 355	09 32 25.87	-11 11 04.8	6.03	K0V	18.3*	+28	<0.1
TWA 6		10 18 28.86	-31 50 03.3	6.89	K7V	~60	+21	0.01
GL 517	HD 118100	13 34 43.19	-08 20 31.3	6.46	K5V	19.8*	+53	0.05
HD 160934		17 38 39.81	+61 14 14.0	7.21	K8V	24.5*	+32	0.1
HD 177996	SAO 229520	19 08 50.45	-42 25 41.5	5.97	K1V	31.8*	-21	0.5
HD 197890	BO Mic	20 47 44.97	-36 35 40.7	7.68	K0V	44.4*	-38	0.1
G 145-43	RE 2131+23	21 31 01.50	+23 20 06.2	6.16	K5V	25.1*	-20	0.1
GL 879	HD 216803	22 56 24.08	-31 33 56.1	3.78	K4V	7.6*	-64	0.2
PS 176		01 19 27.34	-26 21 55.3	8.6	M3	25.5	-83	0.1
GL 207.1	G 99-17	05 33 45.12	+01 56 47.0	7.44	M2.5	14.6	-16	0.1
LH 2026	LP 605-23	08 32 30.28	-01 34 31.1	11.48	M6	19.7	+21	0.1
GL 354.1B		09 32 48.48	+26 59 44.7	8.86	M5.5V	~18	+46	0.2
TWA 7		10 42 30.36	-33 40 17.9	7.44	M4V	~60	+22	0.01
LH 2320	G 44-43	10 52 15.09	+05 55 10.0	8.21	M5	9.9	+55	0.1
LP 263–64		11 03 10.21	+36 39 07.3	9.03	M3.5	23.3	+65	0.1
Steph 932		11 15 54.37	+55 19 51.0	6.49	M0.5V	15.0	+57	0.1
TWA 5	CD -33 7795	11 31 55.40	-34 36 27.3	7.35	M3V	~60	+25	0.01
TWA 8B		11 32 41.37	-26 52 08.8	9.38	M3	~60	+32	0.01
TWA 10		12 35 04.48	-41 36 39.9	8.43	M3	~60	+21	0.01
LP 390–16		18 13 06.37	+26 01 51.8	9.10	M4	16.6	+19	0.1
GL 875.1	LH 3861	22 51 52.87	+31 45 16.6	7.42	M3.5V	14.2*	-25	0.3
GJ 1285	AF Psc	23 31 44.81	-02 44 39.7	10.85	M4	29.2	-59	0.1

*HIPPARCOS determined distances.

^aTWA star distance are based on cluster membership, and otherwise, distance are photometric.

^bThis table was constructed through extensive use of the SIMBAD database.

Table 2. Summary of Point-sources Candidates

	H_{prim} mag	Spec type (prim)	D (pc)	Age (Gyrs)	m_H	Sep "	PA	cpn/ bgd?
HD102982	6.9	G3V	42	< 0.30	10.9	0.9"	28.6	cpn
LP 390-16	9.10	M4	16.6	0.1	14.4	1.45"	226.0	bgd
GL503.2	5.45	G2V	25.7	0.3	10.5	1.55"	354.9	cpn
TWA 5	7.35	M3V	55	0.01	12.2	1.96"	358.8	cpn
TWA 6	6.9	K7V	55	0.01	19.9	2.54"	278.7	bgd
TWA 7	7.4	M4V	55	0.01	16.8	2.47"	142.2	bgd
HR7329	5.03	A0V	47.7	0.01–0.04	11.9	4.17"	166.8	cpn
GL577	6.88	G5V	44.3	0.3	10.9	5.34"	260.6	cpn
HD220140	5.87	G9V	19.7	0.05	7.8	10.85"	216.3	cpn
GL875.1	7.4	M3.5V	14.2	< 0.3	20.2	5.42"	250.4	bgd
HD160934	7.21	K8V	24.5	0.1	16.4	8.69"	234.8	cpn
HD180445	6.84	G8V	41.7	< 0.20	9.9	9.45"	52.5	cpn
					20.8	2.88"	337.0	
					18.7	4.51"	108.3	
					17.8	13.87"	275.6	
					21.4	11.61"	200.7	
LHS 2320	8.2	M5	9.9	0.1	13.5	14.92"	96.9	bgd
					15.9	15.13"	93.6	
RE0723+20	7.19	K5V	23.0	0.2	14.6	5.12"	322.7	bgd
					17.7	9.78"	277.4	
					17.8	13.85"	326.9	
HD177996	5.97	K1V	31.8	0.5	19.6	5.20"	300.9	bgd
					15.6	8.08"	301.1	
					17.9	12.50"	244.2	
GL 207.1	7.4	M2.5	14.6	0.1	18.0, 17.6	4.1.4.2"	197.4,199.1	
					17.7	9.7"	289.6	
HD82443	5.28	K0V	17.8	0.2	16.9	6.86"	195.3	
HR8799	5.33	A5V	39.9	0.01–0.04	21.6	13.71"	15.9	
					20.4	15.68"	114.3	
RE1507+76	7.19	G5V	29.4	0.1	16.6	17.11"	8.3	
HD202917	7.13	G5V	45.9	0.1	18.1	13.62"	230.1	
HD17925	4.22	K1V	10.4	0.1	17.47	15.36"	294.6	
LkHa 264	10.14	K3V	65	0.01	16.8	9.28"	220.4	
					21.0	9.51"	233.4	
GL174	5.75	K3V	13.5	0.06	19.4	14.43"	199.2	
HD197890	7.68	K0V	44.4	< 0.1	17.7	9.04"	20.4	
GL354.1B	8.86	M5.5V	18	0.2	16.51	9.51"	317.0	
GJ 1285	10.85	M4	29.2	0.1	14.8	19.04"	50.4	

¹If a survey star is not found in this list, then there were no point-sources detected in the NICMOS images

²All separations have errors of 0.08"

Table 3. Proper Motion of Primary Stars w/ Followup

Star	μ_α (mas/yr)	μ_δ (mas/yr)	Reference
HD 102982	-0.057	-0.081	Hog et al (2000)
Gl 503.2	0.112	-0.018	Perryman et 1997
Gl 577	-0.121	0.112	Perryman et al 1997
HD 180445	0.099	-0.093	Perryman et al (1997)
HD 220140	0.201	0.072	Perryman et al (1997)
HD 160934	-0.031	0.059	Perryman et al (1997)
LP 390-16	0.207	-0.036	Luyten (1979)
HD 177996	0.023	-0.120	Perryman et al (1997)
Re 0723+20	-0.055	-0.238	Montes et al (2001)
LHS 2320	-0.673	-0.094	Bakos, Sahu,& Nemeth (2002)
Gl 875.1	0.527	-0.050	Perryman et al (1997)
TWA 7	-0.122	-0.029	Hog et al (2000)
TWA 6	-0.060	-0.020	Webb et al (1997)

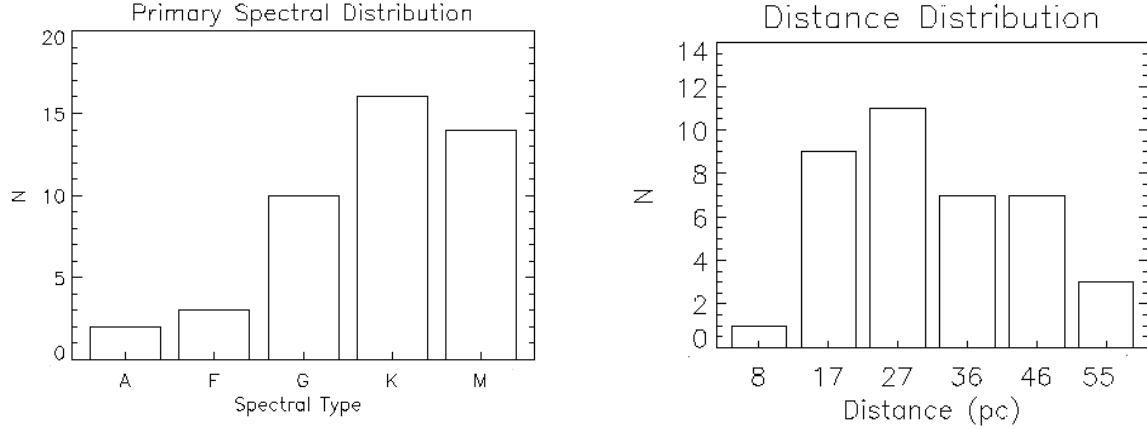


Fig. 1.— The sample consists of a range of spectral types and distances, with a concentration toward lower mass ($<1.0 M_{\odot}$) stars at a median distance of about 30 parsecs. Half of the distances, or 25, were determined by data from the Hipparcos mission.

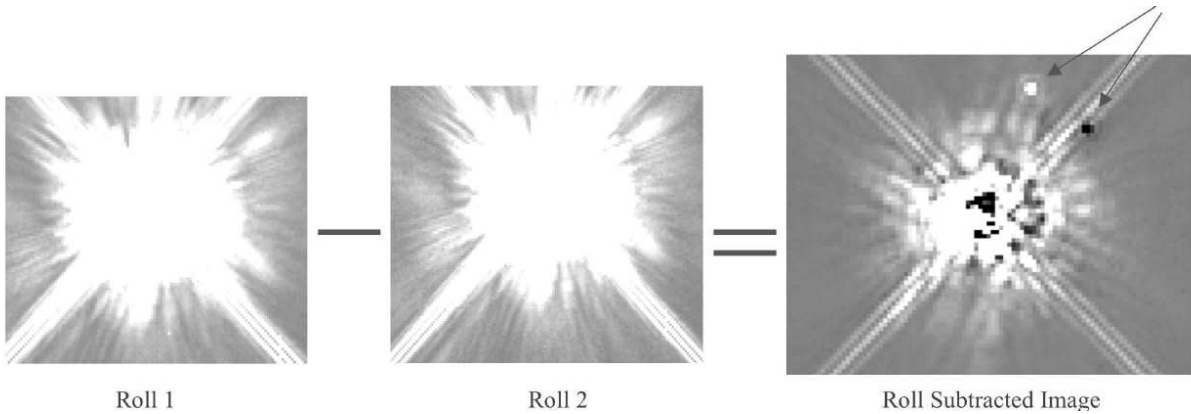


Fig. 2.— The roll subtraction is very effective in eliminating much of the light from the primary star (ex: TWA 7). The star was imaged in the coronagraphic hole (a), the telescope was rolled by 29.9 degrees, and the star was imaged again (b). Subtraction (c) of the two images reveals a stellar-like object approximately $2''$ and 10 mags fainter than the primary. (All three images are stretched from -1 to 1 adu s^{-1} and are approximately the $4'' \times 4''$ around the coronagraph). The object around TWA 7 was found by follow-up observations to not have the same proper motion as the primary.

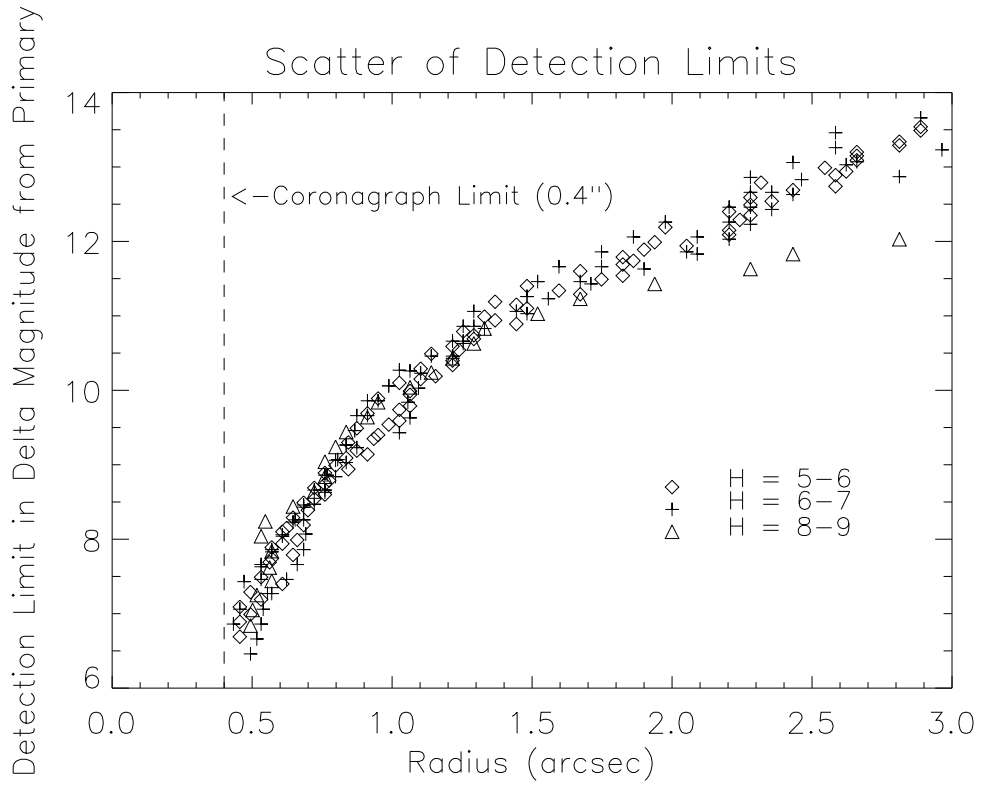


Fig. 3.— Detection limits found by planting and recovering PSF stars in a range of magnitudes within $3''$ of the center of the coronagraph in the roll-subtracted images. Different symbols indicate the different brightness of the primary star plotted.

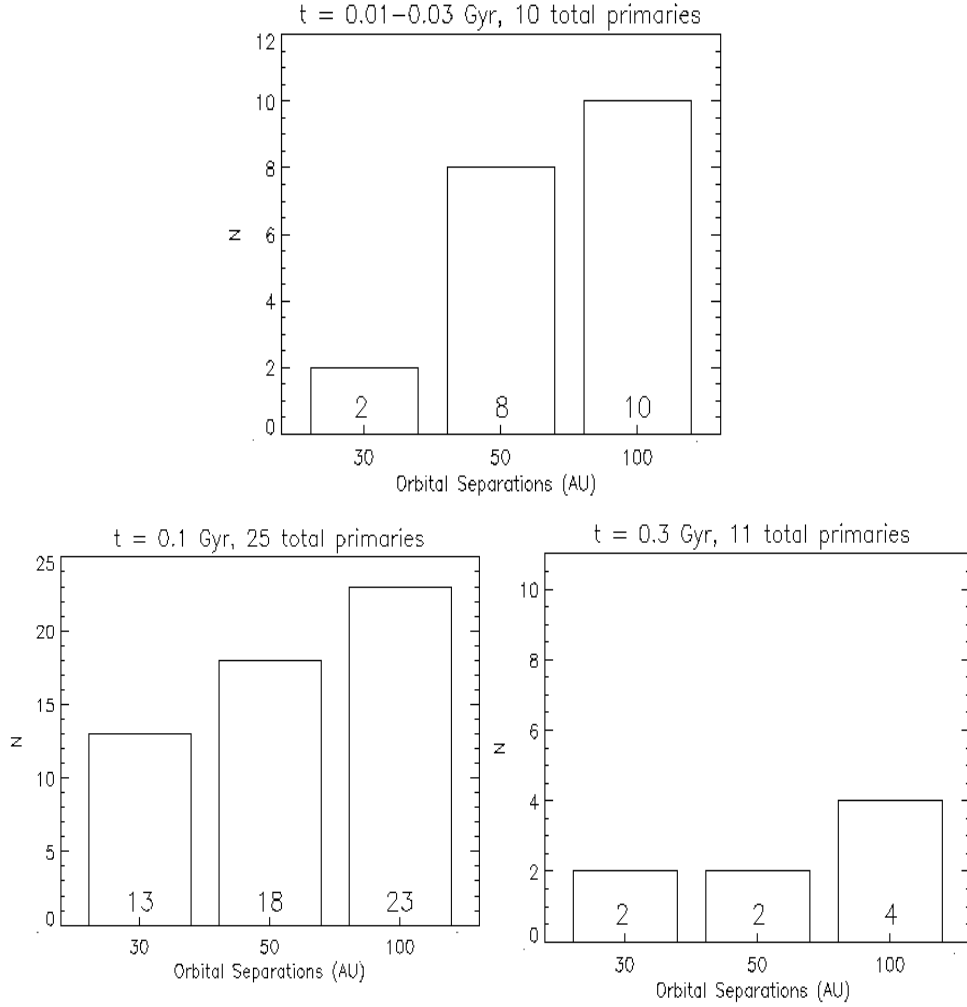


Fig. 4.— The number of primaries, grouped by age, in which a $5 M_{Jupiter}$ object could have been detected at the orbital separations of 30, 50, and 100 AU. Based on the models of Burrows (pers comm), a $5 M_{Jupiter}$ object was assumed to have an absolute H magnitude of 14.2, 16.7, and 18.7 mag, at the ages of 0.02, 0.1, and 0.3 Gyr, respectively. This study explored the high mass planet range above $5 M_{Jupiter}$ around 36%, 61%, and 80% of the 46 primaries at 30, 50, and 100 AU, respectively.

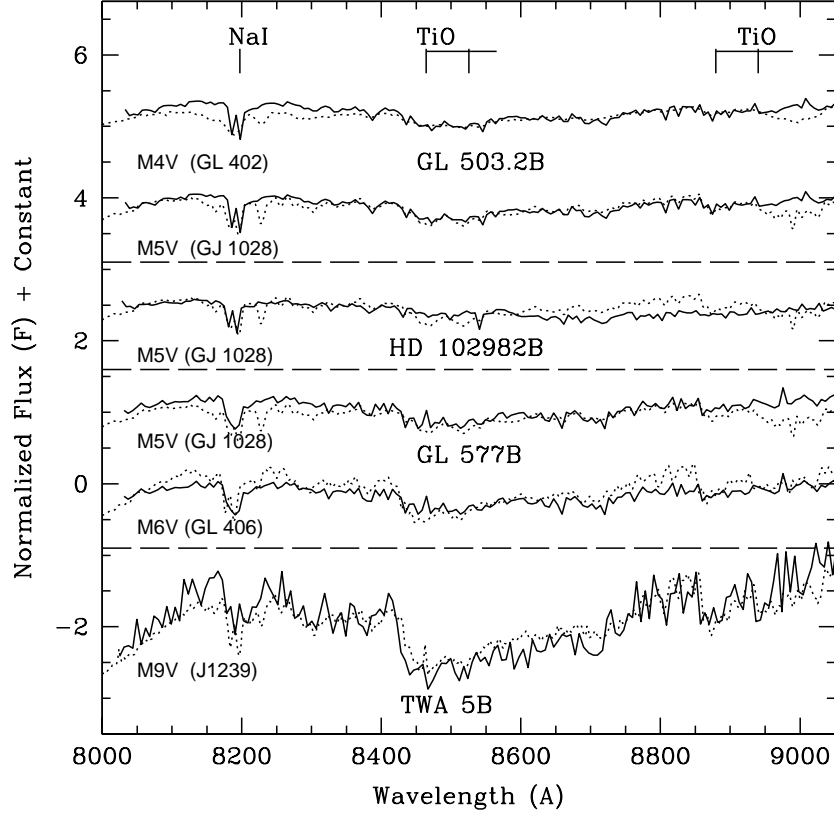


Fig. 5.— STIS spectra of TWA 5B, Gl 577B, HD 102982B and Gl 503.2B (solid) (normalized from $\text{ergs/s/cm}^2/\text{\AA}$) separated by the dashed horizontal lines, compared with standard late-type M dwarf spectra (dashed) (Kirkpatrick et al. 1991; Kirkpatrick et al. 1997). The zero level of each spectrum is -3.3, -1.4, 0.2, 1.3, 2.7 and 4 respectively. The best fitted spectrum was chosen with emphasis on the NaI absorption near 8200\AA and TiO bands near 8450\AA . The best fit appears to lie between M4V and M5V for Gl 503.2B, M5V for HD 102982B, between M5V and M6V for Gl 577B and M9V for TWA 5B. (The longward cutoff of 9050\AA is where the fringing affects the STIS spectrum.)

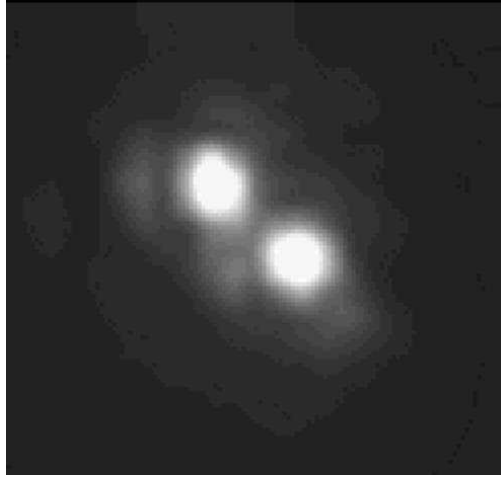


Fig. 6.— Infrared observations of the secondary Gl 577 B & C taken with the AO system at Keck. The measured separation is $0.082''$. The orbit can be measured over several years to get dynamical masses for the two components.

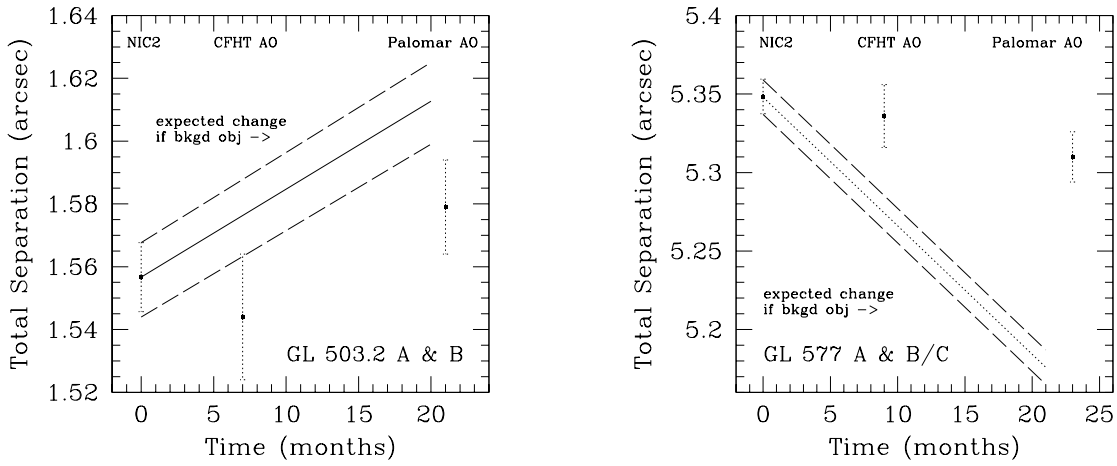


Fig. 7.— Measurements of the separations of two companions (GL 577B/C and GL 503.2) made over the last two years are compared to each other, taking into account a 1 sigma errors bar. The dotted line represents the change in separation expected from the primary’s known proper motion if it was not associated with the candidate companion.

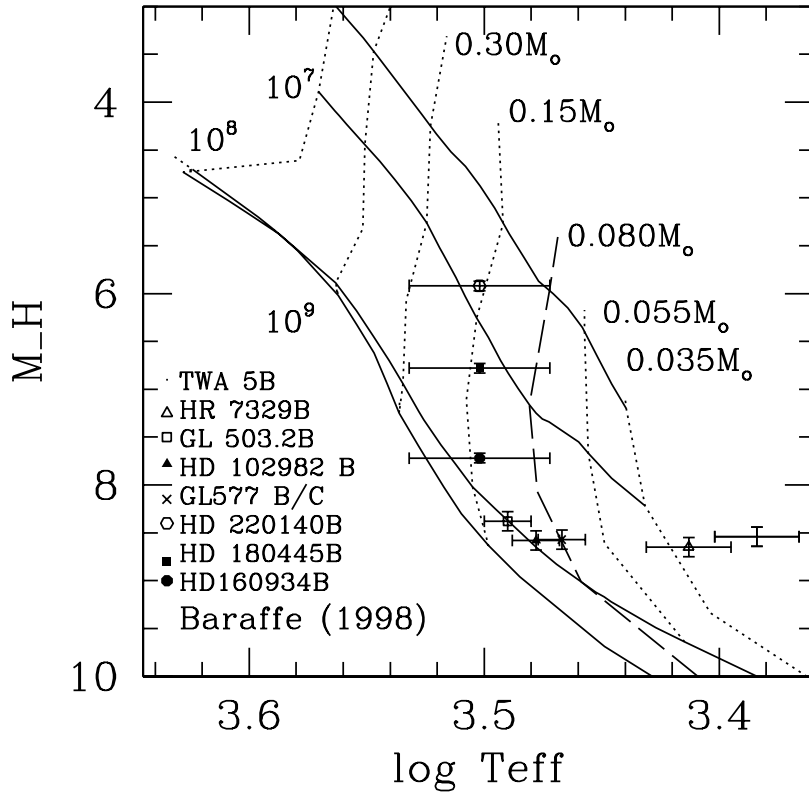


Fig. 8.— H-R diagram of all eight of the discovered companions in this study using the absolute H magnitude determined distances of primary stars and effective temperatures derived from spectra or 2MASS colors. These models (Baraffe et al. 1998) indicate three low mass stars, two very low mass stars, a binary brown dwarf and two brown dwarf companions.

Table A1. Stars from Jeffries (1995)

Star	Sp Type	$v \sin i$ km s ⁻¹	H α (EW) (mÅ)	Li(EW) (mÅ)	log N(Li) ¹
RE 0041+34	K7	15	300	127	1.3
RE 0723+20	K5	12	350	105	1.2
RE 2131+23	K5	70	517	215	1.9

¹Derived from EW Li using Soderblom et al. (1993b)

Table A2. Active M Stars from Reid, Hawley & Gizis (1995)

Star	Sp Type	H α (Å)
Steph 932	M 0.5	2.82
Gl 207.1	M 2.5	7.98
PS176	M 3	7.37
LP263-64	M 3.5	7.83
LP390-16	M 4	10.05
GJ 1285	M 4.5	16.37
LHS2320	M 5	14.47
LHS2026	M 6	21.13

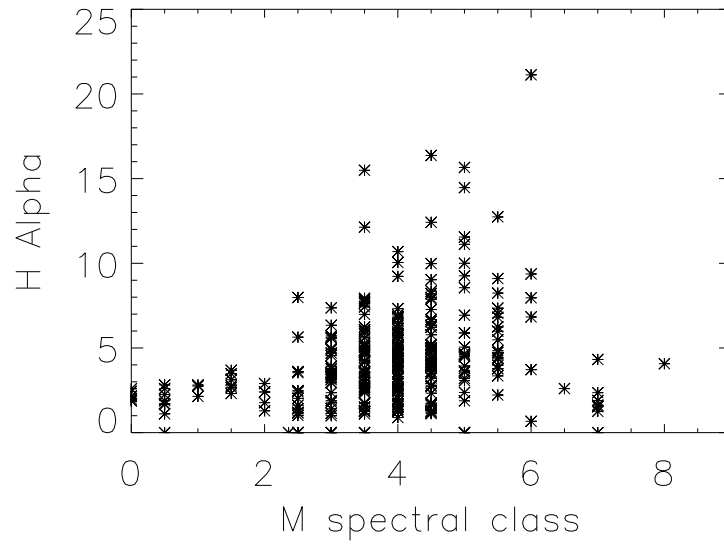


Fig. A1.— The $H\alpha$ measurement plotted against spectral type for those M-type stars with a measurement in Reid, Hawley & Gizis (1995). We took single targets from the top 10% of this distribution across all M spectral classes.